

Pseudo-Goldstone Dark Matter from Primordial Black Holes: Gravitational Wave Signatures and Implications for KM3-230213A Event at KM3NeT

Siyu Jiang^a Fa Peng Huang^{1a}

^aMOE Key Laboratory of TianQin Mission, TianQin Research Center for Gravitational Physics & School of Physics and Astronomy, Frontiers Science Center for TianQin, Gravitational Wave Research Center of CNSA, Sun Yat-sen University (Zhuhai Campus), Zhuhai 519082, China

E-mail: jiangsy36@mail2.sysu.edu.cn, huangfp8@sysu.edu.cn

Abstract. In many well-motivated new physics models, the pseudo-Nambu-Goldstone boson (pNGB) from $U(1)$ symmetry breaking emerges as a promising dark matter candidate. Its coupling, suppressed by the symmetry breaking scale, prevents thermal equilibrium in the early Universe for high scale symmetry breaking. Thus, pNGB dark matter is predominantly produced via non-thermal mechanisms, such as the freeze-in process through a new portal coupling. In this work, we explore a novel mechanism for the production of pNGB dark matter even with feeble Higgs portal coupling—arising from Hawking radiation or superradiance of primordial black holes. We systematically investigate the production of light and heavy pNGB dark matter, both for Schwarzschild and Kerr black holes. We also discuss its potential gravitational wave signatures from domain wall collapse, density perturbations, and Hawking radiation. If the ultraviolet (UV) model is considered, the recent $\mathcal{O}(100)$ PeV neutrino event KM3-230213A at KM3NeT can be naturally explained.

Keywords: dark matter theory, primordial black holes, gravitational waves/sources

¹Corresponding author.

Contents

1	Introduction	1
2	pNGB model	2
3	Schwarzschild Black Holes	4
3.1	Hawking radiation	4
3.2	UV freeze-in	7
3.3	Light pNGB dark matter	8
3.4	Heavy pNGB dark matter	9
4	Kerr Black Holes	10
4.1	Hawking radiation and superradiance	10
4.2	Light pNGB dark matter	11
4.3	Heavy pNGB dark matter	12
5	Gravitational wave	14
5.1	Gravitational wave from domain wall	14
5.2	Induced gravitational wave	17
5.3	Gravitational waves from primordial black hole evaporation	18
6	Possible interpretation of the KM3-230213A neutrino event from pNGB decay	19
7	Conclusions and discussions	22

1 Introduction

Exploring the production mechanism and the microscopic nature of dark matter (DM) remains a central challenge in both cosmology and particle physics. The Standard Model (SM) of particle physics lacks viable DM candidates, necessitating the introduction of new physics beyond the SM. The astrophysical observations, direct detection experiments, and collider searches have placed stringent constraints on fundamental DM properties, such as its mass and interaction cross section. The traditional DM candidate, Weakly Interacting Massive Particles (WIMPs), produced via thermal freeze-out, is increasingly disfavored by direct detection results [1–5]. This situation motivates the exploration of alternative DM candidates and novel production mechanisms.

The pseudo Nambu-Goldstone boson (pNGB) DM associated with U(1) symmetry breaking can naturally evade the severe constraints from direct detection [6–10]. For example, in the case of lepton number symmetry $U(1)_{B-L}$ breaking, the right-handed neutrino gains heavy Majorana mass which can explain the smallness of the neutrino mass via the seesaw mechanism. The Majoron, as the massless Nambu-Goldstone boson (NGB), results in this case. The mass of pNGB appears when introducing an explicit U(1) breaking term which could come from the effect of quantum gravity [11], coupling with another scalar [12–16], neutrino Dirac Yukawa coupling [17], and so on.

Due to the nature of NGB, all couplings of pNGB DM are inversely proportional to the vacuum expectation value (VEV) associated with the $U(1)$ symmetry breaking. Therefore, from this viewpoint, if the breaking scale is high, it seems preferred for pNGB DM to be produced by freeze-in mechanism [18] instead of freeze-out. The DM is assumed to be never in thermal equilibrium with the SM particles. Especially for some TeV-scale and heavier pNGB DM, for which the VEV has to be large enough in order for the DM to be long-lived, it is important to investigate its production mechanism.

Primordial black holes (PBHs), as hypothetical macroscopic objects, may form due to density perturbations following the end of inflation. If a PBH's mass is less than 10^9 g, it would completely evaporate through Hawking radiation before Big Bang nucleosynthesis (BBN). In principle, black holes can efficiently produce any particles with masses below their surface temperature. These particles, with masses significantly exceeding the temperature of the Universe, naturally decouple from thermal equilibrium. This provides a novel mechanism for DM production [19–37], and matter-antimatter asymmetry [38–45]. PBHs may also exhibit memory effects, altering their evolution and impacting DM production [46–48], matter-antimatter asymmetry [49], and gravitational wave (GW) signals [50–52]. In recent years, the production of superheavy DM through superradiance has also attracted considerable attention [53–56].

In this work, we systematically investigate the production of pNGB DM from Schwarzschild and Kerr black holes, considering the effects of Hawking evaporation and superradiance. Furthermore, this DM production mechanism, along with the pNGB DM model, gives rise to a variety of GW signals: 1. GWs from the annihilation of domain walls (DWs) arising from Z_2 symmetry breaking. 2. Induced GWs generated by density perturbations, as PBHs may transiently dominate the Universe before their decay. 3. High-frequency GWs directly emitted from PBHs. Moreover, if pNGB DM mass is around ~ 440 PeV, its decay, facilitated by an ultraviolet (UV) extension of the model, could produce high-energy neutrinos, potentially explaining the KM3-230213A event observed at KM3NeT.

The paper is organized as follows. In section 2, we briefly review the simple pNGB DM model. We review the Hawking radiation of Schwarzschild black holes, the freeze-in production, and discuss the light and heavy pNGB DM separately in section 3. In section 4, we investigate the production of pNGB DM from Kerr black holes, including Hawking radiation and superradiance. The GW signals from DW collapse, density perturbations and the PBH evaporation are given in section 5. Possible interpretation of the neutrino event of KM3-230213A is shown in section 6. Finally, the conclusions and discussions are given in section 7.

2 pNGB model

Firstly, we briefly review the minimal pNGB model. The scalar field S possesses a dark $U(1)_D$ symmetry. The tree-level potential about SM Higgs H and S is

$$V(H, S) = -\frac{\mu_H^2}{2}|H|^2 + \frac{\lambda_H}{2}|H|^4 - \frac{\mu_S^2}{2}|S|^2 + \frac{\lambda_S}{2}|S|^4 + \lambda_{HS}|H|^2|S|^2 - \frac{m^2}{4}(S^2 + S^{*2}) \quad , \quad (2.1)$$

where the first two terms are the potential of the SM Higgs. The term proportional to m^2 is the explicit breaking term, which gives mass to the pNGB χ . The mass of χ can be superheavy, $M_\chi > 100$ TeV, like in the UV model in Refs. [12–15] where the explicit breaking term can be derived by higher symmetry breaking. And in this case the pNGB DM could

decay into neutrinos through scalar mixing or active-sterile neutrino mixing. The signals may interpret the results reported by KM3NeT recently and we will discuss later. After introducing the explicit term, the $U(1)_D$ symmetry is reduced to Z_2 symmetry between $S \rightarrow -S$. There also exists a CP symmetry as $S \rightarrow S^*$ in the potential. After the symmetry breaking, the two scalar fields H and S can be written as

$$H = \frac{1}{\sqrt{2}} \begin{pmatrix} 0 \\ v + h \end{pmatrix}, \quad S = \frac{v_s + s}{\sqrt{2}} e^{i\chi/v_s}, \quad (2.2)$$

where we have used the unitary gauge to eliminate the would-be NGBs in SM Higgs doublet H .

If the mixing coupling λ_{HS} is nonzero, h and s should be diagonalized. However, since we assume $v_s \gg v$, one can ignore the mixing, and just take h and s as physical eigenstate. The stationary conditions of the VEVs are solved as $\mu_S^2 = \lambda_S v_s^2 - m^2$, and after the $U(1)_D$ breaking, the masses of s and χ are given by

$$M_s^2 = \lambda_S v_s^2, \quad M_\chi^2 = m^2. \quad (2.3)$$

We require $\lambda_{HS}, \lambda_S \lesssim 10^{-6}$ so that the dark particles do not come into equilibrium. Then we get $M_s \leq 10^{-3} M_{\text{Pl}}$ for $v_s \leq M_{\text{Pl}}$ where $M_{\text{Pl}} = 1/\sqrt{G_N} \simeq 1.22 \times 10^{19}$ GeV is the Planck mass. Because the vacuum value is real, the CP symmetry is unbroken then the Lagrangian is invariant under $\chi \rightarrow -\chi$, so pNGB is stable and can serve as the DM candidate.

It is worth noticing that when the $U(1)_D$ coincides with the $B - L$ symmetry, the complex singlet S can give Majorana mass to the right-handed neutrinos by introducing the interaction term $S \nu_R^c \nu_R$, through which the traditional seesaw mechanism works. In this case, the pNGB is called Majoron and it can decay into neutrinos through active-sterile neutrino mixing, the decay width reads [57],

$$\Gamma_{\chi \rightarrow \nu\nu} \simeq \frac{1}{10^{19} \text{ s}} \left(\frac{M_\chi}{1 \text{ TeV}} \right) \left(\frac{8 \times 10^{11} \text{ GeV}}{v_s} \right)^2 \left(\frac{\sum_j m_{\nu_j}^2}{2.6 \times 10^{-3} \text{ eV}^2} \right). \quad (2.4)$$

The expression here uses the best fit values of atmospheric and solar mass-splittings [58]. It can be seen that in order to make the Majoron be long-lived, the VEV v_ϕ has to be large enough. In order for Majoron to be a viable DM candidate, its lifetime should be larger than the lifetime of the Universe, $\Gamma_{\chi \rightarrow \nu\nu}^{-1} > \tau_U \sim \mathcal{O}(10^{19})$ sec. For MeV Majoron, the symmetry breaking scale is limited to be larger than $\mathcal{O}(10^{11})$ GeV [59]. Besides, IceCube gives stringer constraint on the lifetime of Majoron DM in the mass range $10^4 \text{ GeV} < M_\chi < 10^9 \text{ GeV}$, $\Gamma_{\chi \rightarrow \nu\nu}^{-1} > \mathcal{O}(10^{28})$ sec [60]. So from Eq. (2.4) the Majoron mass has to be smaller than 10^8 GeV for $v_s \leq M_{\text{Pl}}$. In the case without the Higgs portal, the Majoron DM can be produced by heavy neutrino decay, however, it is found to be too small to satisfy the DM relic density [10, 61, 62].

In this work, we discuss a general class of pNGB DM, rather than focusing solely on Majoron DM. Our study encompasses light DM at the MeV scale as well as superheavy DM with masses exceeding 100 TeV. The light DM scenarios naturally extend to the production of Majoron DM.

Such DM can also be produced via the freeze-in mechanism through the Higgs portal. However, in this work, we propose a novel production mechanism based on Hawking radiation and superradiance from PBHs. Since black hole particle production depends only on gravitational interactions, the pNGB DM can be produced even with feeble portal coupling. The production of pNGB DM can be realized without introducing new interactions.

3 Schwarzschild Black Holes

3.1 Hawking radiation

PBHs may originate from inhomogeneities of density perturbations in the early Universe, with these perturbations potentially arising from cosmic inflation or other alternatives. In this work, we do not focus on the formation mechanisms of PBHs but instead discuss their impact on the Universe after their formation. Assuming the temperature of the Universe at the time of PBH formation is $T = T_{\text{in}}$, the initial mass of the PBH can be expressed in terms of the total radiation energy within a Hubble volume as below [63]

$$M_{\text{in}} \equiv M_{\text{PBH}}(T_{\text{in}}) = \frac{4\pi}{3} \gamma \frac{\rho_r(T_{\text{in}})}{H^3(T_{\text{in}})}, \quad (3.1)$$

where the efficiency factor is $\gamma \simeq (1/\sqrt{3})^3 \simeq 0.2$ [64] at the radiation epoch. Additionally, $\rho_r = \pi^2 g_* T^4/30$ is the radiation energy density of the Universe and $H(T)$ is the Hubble expansion rate,

$$H(T) = \sqrt{\frac{8\pi}{3} \frac{\rho_r}{M_{\text{Pl}}^2}} = \sqrt{\frac{4\pi^3 g_*}{45} \frac{T^2}{M_{\text{Pl}}}}. \quad (3.2)$$

Then we have

$$T_{\text{in}} = \frac{1}{2} \left(\frac{5}{g_* \pi^3} \right)^{1/4} \left(\frac{3\gamma M_{\text{Pl}}^3}{M_{\text{in}}} \right)^{1/2}, \quad (3.3)$$

and from which we get $M_{\text{in}} = \frac{\gamma M_{\text{Pl}}^2}{2H(T_{\text{in}})}$. From Planck data combined with latest BICEP/Keck data, the tensor-to-scalar ratio satisfies $r < 0.036$, namely, the upper limit of Hubble scale during inflation $H(T_{\text{in}}) \leq 5 \times 10^{13} \text{ GeV}$ [65, 66]. Then, we can obtain the lower limit of PBH initial mass $M_{\text{in}} \geq 0.5 \text{ g}$.

We assume a monochromatic mass spectrum of PBHs, such that all PBHs have the same mass after the creation. In general, we typically express the initial energy density of black holes, $\rho_{\text{PBH}}(T_{\text{in}})$, as the ratio of this density to the radiation energy density. This is quantified by introducing the parameter β ,

$$\beta \equiv \frac{\rho_{\text{PBH}}(T_{\text{in}})}{\rho_r(T_{\text{in}})} = \frac{n_{\text{PBH}}(T_{\text{in}}) M_{\text{in}}}{\rho_r(T_{\text{in}})}, \quad (3.4)$$

with $n_{\text{PBH}}(T_{\text{in}})$ being the initial number density of PBHs. The properties of Schwarzschild black holes can be simply described by using only their mass. The relationship between the surface temperature of a Schwarzschild black hole, T_{PBH} , and its mass is given by:

$$T_{\text{PBH}} = \frac{M_{\text{Pl}}^2}{8\pi M_{\text{PBH}}} \simeq 10^{13} \text{ GeV} \left(\frac{1 \text{ g}}{M_{\text{PBH}}} \right). \quad (3.5)$$

Black holes can emit particles through the process of Hawking radiation. For an emitted species i with mass M_i , spin s_i and degrees of freedom g_i , its energy spectrum can be written as [67]

$$\frac{d^2 N_i}{dp dt} = \frac{g_i}{2\pi^2} \frac{\sigma_{s_i}(M_{\text{PBH}}, M_i, p)}{\exp[E_i(p)/T_{\text{PBH}}] - (-1)^{2s_i}} \frac{p^3}{E_i(p)}, \quad (3.6)$$

where $E_i(p) = \sqrt{p^2 + M_i^2}$ denotes the particle energy and σ_{s_i} is the absorption cross section which relates to the greybody factor as $\Gamma_{s_i} \equiv \sigma_{s_i} p^2/\pi$. It can be seen that particles are

efficiently produced via Hawking radiation only when their mass is smaller than the surface temperature of the black hole. After summing over all particle species in the given model, and integrating over the phase space, we can get the evaporation rate of PBH mass,

$$\frac{dM_{\text{PBH}}}{dt} = - \sum_i \int_0^\infty E_i \frac{d^2 N_i}{dp dt} dp = -\varepsilon(M_{\text{PBH}}) \frac{M_{\text{Pl}}^4}{M_{\text{PBH}}^2}, \quad (3.7)$$

where the evaporation function of PBH is defined as $\varepsilon(M_{\text{PBH}}) \equiv \sum_i \varepsilon_i(z_i)$ with $z_i = M_i/T_{\text{PBH}}$. It is interesting to take the approximation $T_{\text{PBH}} \gg M_i$ and geometric limit $\sigma_{s_i} \rightarrow (27\pi M_{\text{PBH}}^2/M_{\text{Pl}}^2)$ [68, 69], from which we can integrate obtain ε_i analytically,

$$\varepsilon_i(z_i) = \frac{27g_i}{8192\pi^5} \int_{z_i}^\infty \frac{x\psi_{s_i}(x, z_i)(x^2 - z_i^2)}{\exp(x) - (-1)^{2s_i}} dx \rightarrow \varepsilon_i(0) = \frac{27g_i}{8192\pi^5} \times \begin{cases} \frac{\pi^4}{15}, & \text{Bosons} \\ \frac{7\pi^4}{120}, & \text{Fermions} \end{cases} \quad (3.8)$$

where $x = E_i/T_{\text{PBH}}$, and $\psi_{s_i} \equiv \sigma_{s_i}/(27\pi M_{\text{PBH}}^2/M_{\text{Pl}}^2)$. So the mass loss rate of a PBH is approximately,

$$\frac{dM_{\text{PBH}}}{dt} = -\varepsilon(M_{\text{PBH}}) \frac{M_{\text{Pl}}^4}{M_{\text{PBH}}^2} \approx -\frac{27}{4} \frac{g_{*\text{PBH}}}{30720\pi} \frac{M_{\text{Pl}}^4}{M_{\text{PBH}}^2}, \quad (3.9)$$

which is consistent with [28]. $g_{*\text{PBH}}$ is the total degree of freedom emitted by the PBH. From this equation we can get

$$M_{\text{PBH}}(t) = M_{\text{in}} \left(1 - \frac{t - t_{\text{in}}}{\tau}\right)^{1/3}, \quad (3.10)$$

with $\tau = \frac{40960\pi}{27g_{*\text{PBH}}} \frac{M_{\text{in}}^3}{M_{\text{Pl}}^4}$ being the PBH lifetime.

Assuming the Universe is always radiation-dominated, utilizing the relationship between the Hubble constant and temperature, along with $H(\tau) = 1/(2\tau)$, the Universe's temperature T_{evap} when PBH evaporates can be determined,

$$T_{\text{evap}} \simeq \frac{9}{128} \left(\frac{1}{5g_*\pi^5}\right)^{1/4} \left(\frac{g_{*\text{PBH}}M_{\text{Pl}}^5}{2M_{\text{in}}^3}\right)^{1/2}. \quad (3.11)$$

During the radiation-dominated era, the energy density of black holes evolves as T^3 , while the radiation energy density evolves as T^4 . Consequently, when β exceeds a critical value $\beta_c \equiv T_{\text{evap}}/T_{\text{in}}$, PBHs will dominate the Universe before their evaporation.

In the case that PBHs dominate the Universe's energy density before they completely evaporate, T_{evap} is determined by setting $H(\tau) = 2/(3\tau)$ and making the replacement $\rho_r \rightarrow M_{\text{in}}n_{\text{PBH}}(T_{\text{evap}}) = M_{\text{in}}n_{\text{PBH}}(T_{\text{in}})T_{\text{evap}}^3/T_{\text{in}}^3$ in Eq. (3.2), then we get

$$T_{\text{evap}}|_{\text{PBHdom}} \simeq \frac{9}{256} \left(\frac{g_{*\text{PBH}}^2}{2\beta}\right)^{1/3} \left(\frac{1}{5^5\pi^{17}g_*^3}\right)^{1/12} \left(\frac{M_{\text{Pl}}^{17}}{3\gamma M_{\text{in}}^{11}}\right)^{1/6}. \quad (3.12)$$

To be consistent with the observational results of BBN, we require the initial mass of PBHs to be less than $\sim 10^9$ g such that they fully evaporate before BBN. Furthermore, if PBHs dominate the Universe prior to their evaporation, they may generate a significant amount of induced GWs, contributing additional radiation energy density and thus impacting BBN observations. The constraint on the initial fraction is given by [70]

$$\beta \lesssim 1.1 \times 10^{-6} \left(\frac{\gamma}{0.2}\right)^{-1/2} \left(\frac{M_{\text{in}}}{10^4 \text{ g}}\right)^{-17/24}. \quad (3.13)$$

In the massless limit and geometric limit, the production rate of particle species i is

$$\Gamma_{\text{PBH} \rightarrow i} \equiv \frac{dN_i}{dt} = \frac{27g_i M_{\text{Pl}}^2}{1024\pi^4 M_{\text{PBH}}} \begin{cases} 2\zeta(3), & \text{Bosons} \\ \frac{3}{2}\zeta(3), & \text{Fermions} \end{cases}. \quad (3.14)$$

For any particle i , by using $\int dt = \int dM_{\text{PBH}} (dM_{\text{PBH}}/dt)^{-1}$, if the initial PBH temperature T_{in} is larger than the mass M_i where we assume i is a boson,

$$N_i = \int_0^{M_{\text{in}}} \frac{1}{\varepsilon(M_{\text{PBH}})} \frac{M_{\text{PBH}}^2}{M_{\text{Pl}}^4} \frac{27g_i \zeta(3) M_{\text{Pl}}^2}{512\pi^4 M_{\text{PBH}}} dM_{\text{PBH}} = \frac{120\zeta(3)}{\pi^3} \frac{g_i}{g_{*\text{PBH}}} \left(\frac{M_{\text{in}}}{M_{\text{Pl}}} \right)^2. \quad (3.15)$$

While, if $T_{\text{in}} < M_i$, the PBH can radiate i only when the PBH temperature raises to exceed M_i ,

$$N_i = \int_0^{\frac{M_{\text{Pl}}^2}{8\pi M_i}} \frac{1}{\varepsilon(M_{\text{PBH}})} \frac{M_{\text{PBH}}^2}{M_{\text{Pl}}^4} \frac{27g_i \zeta(3) M_{\text{Pl}}^2}{512\pi^4 M_{\text{PBH}}} dM_{\text{PBH}} = \frac{15\zeta(3)}{8\pi^5} \frac{g_i}{g_{*\text{PBH}}} \left(\frac{M_{\text{Pl}}}{M_i} \right)^2, \quad (3.16)$$

if i is a fermion, the above expressions have to be multiplied by $3/4$.

If the PBHs dominate the energy density of the Universe before evaporation, the radiation into SM particles will reheat the Universe and dilute the final DM relic. The dilution factor can be derived by using the conservation of energy before and after the evaporation of PBHs [44],

$$\frac{\pi^2}{30} g_* T_{\text{evap}}^4 + M_{\text{in}} \frac{n_{\text{PBH}}(T_{\text{in}})}{s(T_{\text{in}})} s(T_{\text{evap}}) = \frac{\pi^2}{30} g_* \tilde{T}_{\text{evap}}^4, \quad (3.17)$$

from which we get

$$\frac{s(\tilde{T}_{\text{evap}})}{s(T_{\text{evap}})} = \left(\frac{\tilde{T}_{\text{evap}}}{T_{\text{evap}}} \right)^3 = \left(1 + \frac{\beta T_{\text{in}}}{T_{\text{evap}}} \right)^{3/4}, \quad (3.18)$$

where $s(T)$ is the entropy density and \tilde{T}_{evap} is the temperature of the SM plasma after PBH evaporation occurs. The PBHs come to dominate the Universe's energy density before they evaporate if the second factor in the bracket exceeds unity. Then the particle number density produced from PBHs is diluted and reads,

$$Y_i \equiv \frac{N_i n_{\text{PBH}}(T_{\text{evap}})}{s(T_{\text{evap}})} \frac{s(T_{\text{evap}})}{s(\tilde{T}_{\text{evap}})} = \frac{N_i n_{\text{PBH}}(T_{\text{in}})}{s(T_{\text{in}})} \frac{s(T_{\text{evap}})}{s(\tilde{T}_{\text{evap}})} = \frac{3\beta T_{\text{in}} N_i}{4M_{\text{in}}} \frac{s(T_{\text{evap}})}{s(\tilde{T}_{\text{evap}})}. \quad (3.19)$$

The relic density of the particle i at present is

$$\Omega_i^{\text{evap}} = \frac{\rho_i}{\rho_c} = \frac{M_i}{\rho_c} \frac{n_i}{s}(t_0) s_0 = \frac{M_i}{\rho_c} Y_i s_0, \quad (3.20)$$

where $\rho_c \simeq 4.78 \times 10^{-6} \text{ GeV cm}^{-3}$ and $s_0 \simeq 2891.2 \text{ cm}^{-3}$ [71] are the present critical energy density and entropy density, respectively. In summary, if there is no PBH dominated period, namely, $\beta < \beta_c$, the relic density can be obtained as

$$\Omega_i^{\text{evap}} \simeq 1.64 \times 10^6 \beta g_i \left(\frac{g_*}{100} \right)^{-1/4} \left(\frac{g_{*\text{PBH}}}{100} \right)^{-1} \left(\frac{M_{\text{in}}}{M_{\text{Pl}}} \right)^{1/2} \left(\frac{M_i}{\text{GeV}} \right), \quad M_i < \frac{M_{\text{Pl}}^2}{8\pi M_{\text{in}}}, \quad (3.21)$$

$$\simeq 2.59 \times 10^3 \beta g_i \left(\frac{g_*}{100} \right)^{-1/4} \left(\frac{g_{*\text{PBH}}}{100} \right)^{-1} \left(\frac{M_{\text{Pl}}^7}{M_{\text{in}}^3 M_i^4} \right)^{1/2} \left(\frac{M_i}{\text{GeV}} \right), \quad M_i > \frac{M_{\text{Pl}}^2}{8\pi M_{\text{in}}}. \quad (3.22)$$

While, if the initial energy fraction of PBH is large enough, namely, $\beta > \beta_c$, the corresponding relic density reads,

$$\Omega_i^{\text{evap}} \simeq 6.12 \times 10^5 g_i \left(\frac{g_*}{100} \right)^{-1/4} \left(\frac{g_{* \text{PBH}}}{100} \right)^{-1/2} \left(\frac{M_{\text{Pl}}}{M_{\text{in}}} \right)^{1/2} \left(\frac{M_i}{\text{GeV}} \right), \quad M_i < \frac{M_{\text{Pl}}^2}{8\pi M_{\text{in}}}, \quad (3.23)$$

$$\simeq 0.97 \times 10^3 g_i \left(\frac{g_*}{100} \right)^{-1/4} \left(\frac{g_{* \text{PBH}}}{100} \right)^{-1/2} \left(\frac{M_{\text{Pl}}^9}{M_{\text{in}}^5 M_i^4} \right)^{1/2} \left(\frac{M_i}{\text{GeV}} \right), \quad M_i > \frac{M_{\text{Pl}}^2}{8\pi M_{\text{in}}}. \quad (3.24)$$

It is interesting to notice that when PBHs dominate the energy density of the early Universe before they evaporate, the relic density is independent of β .

3.2 UV freeze-in

In addition to being produced via Hawking evaporation, we note that in the model, when λ_{HS} is nonzero, DM can also be generated through the freeze-in mechanism via the Higgs portal $HH \rightarrow s \rightarrow \chi + \chi$. The decay width of the scalar field s is [62],

$$\Gamma_{s \rightarrow H^\dagger H} = \frac{\lambda_{HS}^2 M_s}{8\pi \lambda_S} \sqrt{1 - \frac{4M_h^2}{M_s^2}}, \quad \Gamma_{s \rightarrow \chi\chi} = \frac{\lambda_S M_s}{32\pi} \sqrt{1 - \frac{4M_\chi^2}{M_s^2}}. \quad (3.25)$$

with $M_h \simeq 125$ GeV being the mass of SM Higgs. During freeze-in, the Boltzmann equation for the pNGB DM is given by [61, 62]

$$\frac{dY_\chi(x)}{dz} = \frac{2}{s(z)H(z)z} \gamma_{\chi\chi \rightarrow H^\dagger H}, \quad (3.26)$$

where $z = M_\chi/T$ and $\gamma_{\chi\chi \rightarrow H^\dagger H}$ is the interaction rate,

$$\gamma_{\chi\chi \rightarrow H^\dagger H} \equiv \frac{g_H}{2!2!} \frac{T \lambda_{HS}^2}{2^9 \pi^5} \int_{4M_\chi^2}^{\infty} ds \sqrt{s - 4M_\chi^2} K_1(\sqrt{s}/T) \frac{s^2}{(s - M_s^2)^2} \simeq \frac{3\lambda_{HS}^2 T^8}{2\pi^5 M_s^4}. \quad (3.27)$$

with g_H being the degree of freedom of SM Higgs. Assuming the DM begins to be produced at plasma temperature T_{reh} , in the UV Freeze-in scheme, $M_s \gg T_{\text{reh}}$,

$$\Omega_\chi^{\text{FI}} = 3.34 \times 10^{22} \lambda_{HS}^2 \left(\frac{100}{g_s} \right) \left(\frac{100}{g_*} \right)^{1/2} \left(\frac{T_{\text{reh}}}{M_s} \right)^4 \left(\frac{M_\chi}{T_{\text{reh}}} \right). \quad (3.28)$$

We choose $\lambda_{HS} = 10^{-7}$, $M_s = 10 T_{\text{reh}}$ and $T_{\text{reh}} = T_{\text{in}}$ when considering UV freeze-in in this work. We also have to multiply it with the dilution factor $\left(1 + \beta \frac{T_{\text{in}}}{T_{\text{evap}}}\right)^{-3/4}$ when we take into account the reheating from PBHs if the PBHs dominate the Universe before they evaporate. When $M_s \ll T_{\text{in}}$, the pNGB DM could also be produced by IR freeze-in and the relic reads [62],

$$Y_\chi^{\text{IR}} \approx \frac{405\sqrt{10}}{(2\pi)^5} \frac{\text{Br}_{s \rightarrow \chi\chi} \lambda_{HS}^2 M_{\text{Pl}}}{g_{*s} g_*^{1/2} \lambda_S M_s} \sqrt{1 - \frac{4M_h^2}{M_s^2}}. \quad (3.29)$$

where $\text{Br}_{s \rightarrow \chi\chi} = \Gamma_{s \rightarrow \chi\chi} / (\Gamma_{s \rightarrow H^\dagger H} + \Gamma_{s \rightarrow \chi\chi})$ is the branch ratio of the decay of s into the DM. It can be seen that the result does not depend on the initial temperature T_{in} , so this contribution can dominate over the PBH evaporation if we fine-tune the coupling λ_{HS} . However,

in this work we focus on the DM production from PBH so we only consider the UV freeze-in where $M_s > T_{\text{in}}$. It is worth noting that PBHs can not only directly produce DM but can also generate intermediate mediators s , which subsequently decay into two DM particles. We require $\lambda_s \leq 10^{-6}$ and $v_s \leq M_{\text{Pl}}$ where the former condition comes from the non-equilibrium of DM. So the scalar mass should satisfy $M_s \leq 10^{-3} M_{\text{Pl}}$. From this and $M_s = 10 T_{\text{in}}$ we get $M_{\text{in}} \gtrsim 3 \text{ g}$.

Thus, in general, the final DM relic density is

$$\Omega_{\text{DM}} = \Omega_{\chi}^{\text{evap}} + 2\text{Br}_{s \rightarrow \chi\chi} \Omega_s^{\text{evap}} + \Omega_{\chi}^{\text{FI}}. \quad (3.30)$$

In the following, we will use this formula to consider two different scenarios for DM production, namely, the light pNGB DM and heavy pNGB DM. The present DM relic abundance satisfies $\Omega_{\text{DM}} h^2 \simeq 0.12$ where the dimensionless Hubble parameter $h \approx 0.67$.

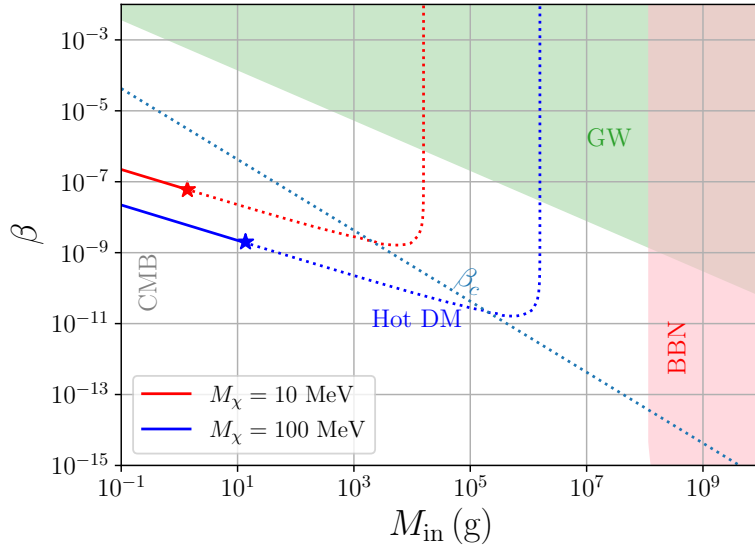


Figure 1. Contours showing the parameter space where PBHs produce the correct relic abundance of DM. The red and blue curves correspond to DM masses of 10 MeV and 100 MeV, respectively. The star marks the critical black hole mass above which the evaporated DM particles are hot DM. Gray, green, and red regions represent excluded regions from CMB observations, excessive GW, and BBN, respectively.

3.3 Light pNGB dark matter

Firstly, we consider the case of light DM with mass $M_{\chi} = 10 \text{ MeV}$ and 100 MeV . The DM relic density in these cases is given by Eqs. (3.21) and (3.23). We find that the freeze-in contribution is negligible.

For light DM, radiated DM may be too hot. We must carefully examine its velocity to determine whether it is excluded by large-scale structure observation. We can simply follow the discussions on the constraints of warm DM. The average DM velocity today V_0 is given by [40]

$$V_0 = \frac{a_{\text{evap}}}{a_0} \frac{\langle p_{\chi}^{\text{evap}} \rangle}{M_{\chi}} \simeq \frac{a_{\text{evap}}}{a_{\text{eq}}} \frac{a_{\text{eq}}}{a_0} \frac{\langle E_{\chi}^{\text{evap}} \rangle}{M_{\chi}}, \quad (3.31)$$

where $\langle p_\chi^{\text{evap}} \rangle$ and $\langle E_\chi^{\text{evap}} \rangle$ are the averaged momentum and averaged energy of DM at evaporation, respectively. a_{evap} is the scale factor after PBH evaporation. a_0 and a_{eq} are the scale factor at present and matter-radiation equality, respectively. Note that we have the relation

$$\frac{a_{\text{evap}}}{a_{\text{eq}}} \simeq \frac{T_{\text{eq}}}{\tilde{T}_{\text{evap}}} \left[\frac{g_{*s}(T_{\text{eq}})}{g_{*s}(\tilde{T}_{\text{evap}})} \right]^{\frac{1}{3}}, \quad \frac{a_{\text{eq}}}{a_0} \simeq \frac{\Omega_r}{\Omega_m} \approx 3 \times 10^{-4}. \quad (3.32)$$

Then the main task is to calculate the averaged energy of pNGB DM which is produced by PBH evaporation.

$$\langle E_\chi^{\text{evap}} \rangle = \frac{1}{N_\chi} \int E_\chi \frac{dN_\chi}{dp dt} dp dt \simeq \frac{\pi^3}{120\zeta(3)} \frac{g_{* \text{PBH}}}{g_\chi} \frac{M_{\text{Pl}}^2}{M_{\text{in}}^2} \int \frac{dM_{\text{PBH}}}{dt} \frac{g_\chi}{g_{* \text{PBH}}} dt \approx 5.4 \left(\frac{M_{\text{Pl}}^2}{8\pi M_{\text{in}}} \right). \quad (3.33)$$

In the second equality we have used Eq. (3.7) and the fact that all particles including DM are lighter than the Hawking temperature of PBHs. The value of the prefactor is close to 6 given by [22] and 6.3 by [28]. By using $V_0 \lesssim 1.8 \times 10^{-8}$ from the upper limits of the warm DM velocity [27],

$$M_\chi > 7.3 \times 10^{-3} \text{ GeV} \times \left(\frac{M_{\text{in}}}{1 \text{ g}} \right). \quad (3.34)$$

The results are shown in Fig. 1, where the star denotes the critical black hole mass. For black holes exceeding the critical mass, the produced DM becomes too hot to satisfy the constraint from large-scale structure formation. The gray region is from the CMB constraint and the green region is from Eq. (3.13). The pink region represents the BBN constraint which is taken from the most recent result [72].

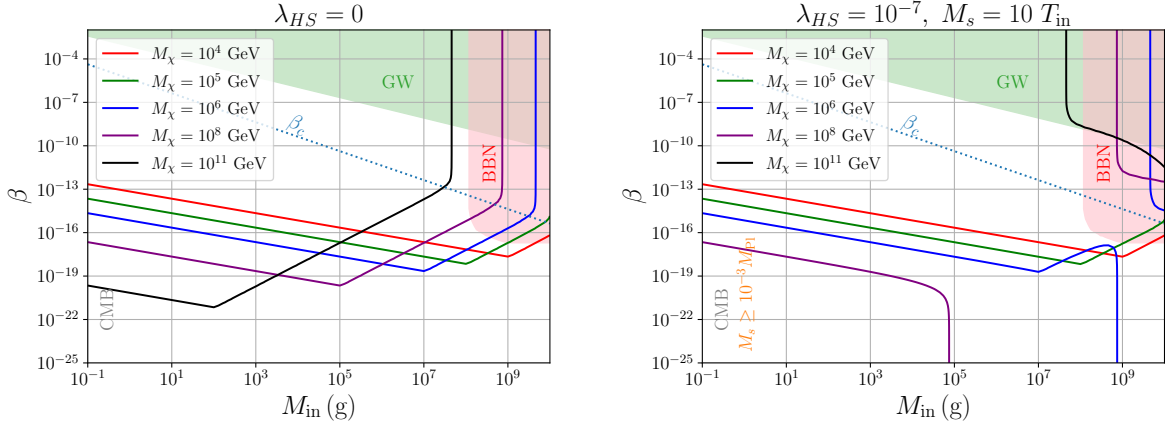


Figure 2. Contour plot for heavy pNGB DM. The left panel shows the scenario where DM is entirely produced through the evaporation of Schwarzschild PBHs, without considering the contribution from UV freeze-in. The right panel includes the contribution from UV freeze-in. For the UV freeze-in process, we choose $\lambda_{HS} = 10^{-7}$ and $M_s = 10 T_{\text{in}}$.

3.4 Heavy pNGB dark matter

For the heavy pNGB DM case, we show the main results in Fig. 2. In the left panel, we show the results without UV freeze-in. The red, green, blue, purple, and black lines correspond to

pNGB masses of 10^4 , 10^5 , 10^6 , 10^8 , and 10^{11} GeV, respectively. The decrease of β with M_{in} is described by Eq. (3.21), where $\beta \propto (M_{\text{in}}/\text{GeV})^{-1/2}$. And then, when the initial PBH mass is larger, the DM relic density satisfies Eq. (3.21) where $\beta \propto (M_{\text{in}}/\text{GeV})^{3/2}$. When $\beta > \beta_c$ the PBHs dominate the Universe and the relic density is independent of β . In the right panel, we include the UV freeze-in with $\lambda_{HS} = 10^{-7}$. The orange region does not satisfy the condition that $M_s \leq 10^{-3} M_{\text{Pl}}$ for $\lambda_S \leq 10^{-6}$ and $v_s \leq M_{\text{Pl}}$. The UV freeze-in dominates when the M_{in} is larger, or in other words, when the T_{in} is lower.

4 Kerr Black Holes

4.1 Hawking radiation and superradiance

Kerr black holes, due to their non-zero angular momentum, alter their surface temperature and radiation rate and also the spectrum of Hawking radiation. This deviation from the static Schwarzschild case provides a new perspective for understanding quantum effects in strong gravitational fields. For the case of Kerr black holes, the horizon temperature reads,

$$T_{\text{PBH}} = \frac{M_{\text{Pl}}^2}{4\pi M_{\text{PBH}}} f(a_\star) = \frac{M_{\text{Pl}}^2}{4\pi M_{\text{PBH}}} \frac{\sqrt{1-a_\star}}{1 + \sqrt{1-a_\star}}, \quad (4.1)$$

where $a_\star \equiv JM_{\text{Pl}}^2/M_{\text{PBH}}^2$, with J denoting the angular momentum of PBHs. The case with $a_\star = 0$ corresponds to the Schwarzschild limit. The energy spectrum now explicitly depends on the angular quantum numbers l and m [67],

$$\frac{d^2 N_i}{dp dt} = \frac{g_i}{2\pi^2} \sum_{l=s_i}^l \sum_{m=-l}^l \frac{\sigma_{s_i}^{lm}(M_{\text{PBH}}, p, a_\star)}{\exp[(E_i(p) - m\Omega)/T_{\text{PBH}}] - (-1)^{2s_i}} \frac{p^3}{E_i(p)}, \quad (4.2)$$

with $\Omega = (a_\star M_{\text{Pl}}^2/(2M_{\text{PBH}})) \left(1/\left(1 + \sqrt{1-a_\star^2}\right)\right)$ being the horizon angular velocity.

For Kerr black holes, due to the NGB nature, pNGB DM can be produced not only via Hawking radiation but also through black hole superradiance. The superradiance of DM happens when the Compton length of the DM particle $\lambda_C = 1/M_\chi$ is comparable with the gravitational radius $r_g = M_{\text{PBH}}/M_{\text{Pl}}^2$. The superradiance process is efficient when $\alpha \equiv r_g/\lambda_C \sim \mathcal{O}(1)$. Considering the dominant unstable mode with quantum number $n = 2$ and $l = m = 1$, the superradiance rate Γ_{SR} can be approximated by the Detweiler formalism [73],

$$\Gamma_{\text{SR}} = \frac{M_\chi}{24} \left(\frac{M_{\text{PBH}} M_\chi}{M_{\text{Pl}}^2} \right)^8 (a_\star - 2M_\chi r_+) , \quad (4.3)$$

where $r_+ = M_{\text{PBH}} \left(1 + \sqrt{1-a_\star^2}\right)/M_{\text{Pl}}^2$ represents the event horizon. It is clear that Γ_{SR} vanishes in the limit $a_\star \rightarrow 0, r_+ \rightarrow 0$. This approximation fails in the large α regime, where we need to solve the Klein-Gordon equation on the Kerr background numerically. However, the analytic expression Eq. (4.3) is enough for qualitative analysis. Therefore, for the PBH with $M_{\text{PBH}} \lesssim 10^9$ g, only heavy pNGB with $M_\chi \gtrsim 10^4$ GeV will get contribution from superradiance.

The final amount of DM particles $N_\chi^{\text{SR}}(\text{end})$ per PBH after the superradiance is easy to obtain [53],

$$N_\chi^{\text{SR}}(\text{final}) \simeq 1.5 \times 10^{19} \left(\frac{M_{\text{in}}}{10^5 \text{ g}} \right)^2 \left(a_\star^{\text{in}} - a_\star^{\text{end}} \right) \simeq \mathcal{O}(10^{18}) \left(\frac{M_{\text{in}}}{10^5 \text{ g}} \right)^2. \quad (4.4)$$

The typical timescale for superradiance

$$t_{\text{SR}} \sim \frac{1}{\Gamma_{\text{SR}}} \simeq \frac{24}{M_\chi} \left(\frac{M_{\text{Pl}}^2}{M_{\text{in}} M_\chi} \right)^8 \frac{1}{a_\star^{\text{in}}} . \quad (4.5)$$

For the DM production from Kerr black hole, we need to perform numerical calculations. In the following, we define

$$\mathcal{N}_\chi = n_\chi a^3, \quad \varrho_{\text{PBH}} = \rho_{\text{PBH}} a^3, \quad \varrho_r = \rho_r a^4 . \quad (4.6)$$

which can help to simplify the Boltzmann equations.

4.2 Light pNGB dark matter

Unlike the Schwarzschild black holes, for Kerr black holes we cannot derive approximately analytic results. Instead, we have to solve the evolution equations of PBHs numerically. For light DM, since superradiance is ineffective in this case, we only need to consider black hole evolution and DM production driven by Hawking radiation. From Eq. (4.2) we get,

$$H a \frac{dM_{\text{PBH}}}{da} = -\varepsilon(M_{\text{PBH}}, a_\star) \frac{M_{\text{Pl}}^4}{M_{\text{PBH}}^2} \quad (4.7)$$

$$H a \frac{da_\star}{da} = -a_\star [\gamma(M_{\text{PBH}}, a_\star) - 2\varepsilon(M_{\text{PBH}}, a_\star)] \frac{M_{\text{Pl}}^4}{M_{\text{PBH}}^3} , \quad (4.8)$$

$$H a \frac{d\mathcal{N}_\chi^{\text{PBH}}}{da} = \frac{\varrho_{\text{PBH}}}{M_{\text{PBH}}} \Gamma_{\text{PBH} \rightarrow \chi} , \quad (4.9)$$

where $\varepsilon(M_{\text{PBH}}, a_\star)$ and $\gamma(M_{\text{PBH}}, a_\star)$ are given by

$$\begin{aligned} \varepsilon(M_{\text{PBH}}, a_\star) &\equiv \sum_i \varepsilon_i(z_i, a_\star) = \frac{27}{8192\pi^5} \sum_i \int_{z_i}^\infty \sum_{l,m} \frac{\psi_{s_i}^{lm}(x, a_\star) (x^2 - z_i^2)}{\exp(x'/2f(a_\star)) - (-1)^{2s_i}} x \, dx \\ \gamma(M_{\text{PBH}}, a_\star) &\equiv \sum_i \gamma_i(z_i, a_\star) = \frac{27}{1024\pi^4} \sum_i \int_{z_i}^\infty \sum_{l,m} \frac{m \psi_{s_i}^{lm}(x, a_\star) (x^2 - z_i^2)}{\exp(x'/2f(a_\star)) - (-1)^{2s_i}} dx , \end{aligned} \quad (4.10)$$

with $x' = x - m\Omega'$, where $x = 8\pi M_{\text{PBH}} E_i / M_{\text{Pl}}^2$, $\Omega' = \Omega / T_{\text{PBH}}$.

It is also required to write down the evolution equations of the radiation energy of the Universe and the total energy of PBHs as

$$\frac{d\varrho_r}{da} = -\frac{\varepsilon_{\text{SM}}(M_{\text{PBH}}, a_\star)}{\varepsilon(M_{\text{PBH}}, a_\star)} \frac{1}{M_{\text{PBH}}} \frac{dM_{\text{PBH}}}{da} a \varrho_{\text{PBH}} , \quad (4.11)$$

$$\frac{d\varrho_{\text{PBH}}}{da} = \frac{1}{M_{\text{PBH}}} \frac{dM_{\text{PBH}}}{da} \varrho_{\text{PBH}} , \quad (4.12)$$

$$H^2 = \frac{8\pi}{3M_{\text{Pl}}^2} (\varrho_{\text{PBH}} a^{-3} + \varrho_r a^{-4}) . \quad (4.13)$$

where ε_{SM} only includes the contributions from SM particles. The source terms on the right-hand side of the first and second lines are provided by PBH Hawking radiation and superradiance. The third line represents the Hubble rate of cosmic expansion. Besides, we also have to track the evolution of the temperature of the Universe [74–76],

$$\frac{dT}{da} = -\frac{T}{\Delta} \left\{ \frac{1}{a} + \frac{\varepsilon_{\text{SM}}(M_{\text{PBH}}, a_\star)}{\varepsilon(M_{\text{PBH}}, a_\star)} \frac{1}{M_{\text{PBH}}} \frac{dM_{\text{PBH}}}{da} \frac{g_*(T)}{g_{*s}(T)} \frac{a \varrho_{\text{PBH}}}{4\varrho_r} \right\} , \quad (4.14)$$

where

$$\Delta = 1 + \frac{T}{3g_{*s}(T)} \frac{dg_{*s}(T)}{dT} \quad (4.15)$$

takes into account the variation of the degree of freedoms.

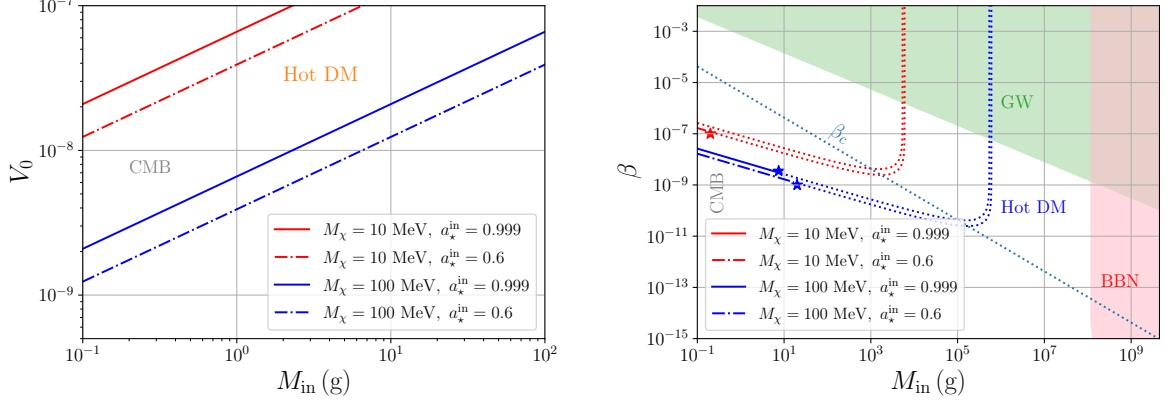


Figure 3. Left panel: The present averaged velocity of DM particles evaporated from PBHs. The orange region represents exclusions from Lyman- α observations. Right panel: Contour plot for the relic density of light pNGB DM in the case of Kerr black holes. The stars represent the critical values of PBH mass beyond which the DM is too hot to satisfy the large scale structure.

We solve Eqs. (4.7)-(4.9) and Eqs. (4.11)-(4.14) to obtain the PBHs' evolution. Then we can get

$$\langle E_\chi^{\text{evap}} \rangle = \frac{1}{N_\chi} \int_{t_{\text{in}}}^{t_{\text{evap}}} E_\chi \frac{dN_\chi}{dp dt} dp dt \simeq \frac{\int dt \varepsilon_\chi(M_\chi/T_{\text{PBH}}, a_\star) M_{\text{Pl}}^4 M_{\text{PBH}}^{-2}}{\int dt \Gamma_{\text{PBH} \rightarrow \chi}(M_{\text{PBH}}, a_\star)}, \quad (4.16)$$

where t_{evap} and the evolution of PBHs are given by solving the differential equations numerically. Then we can integrate the right side to get the averaged energy, which is substituted in Eq (3.31) to get the present velocity of DM.

In the left panel of Fig. 3 we show the averaged velocity for different values of DM mass and initial angular momentum of PBHs, as functions of the PBH initial mass. We can see that the 10 MeV pNGB DM is totally excluded by combined constraints from CMB and large scale structure. The averaged velocity is enhanced for larger PBH mass and larger angular momentum. The right panel in Fig. 3 shows the contour plot of DM relic density. It can be seen that the shapes are only slightly different from the results in Fig. 1, demonstrating the validity of the analytical results.

4.3 Heavy pNGB dark matter

Now we consider the production of heavy DM. The main difference is that, in this case, the pNGB DM is produced not only by the Hawking evaporation but also the superradiance. It has been shown in Ref. [53] that the superradiant production enhances the DM relic density by a factor of $\mathcal{O}(10)$. The superradiant production has also been used for the leptogenesis mechanism [54] and the production of dark radiation [55].

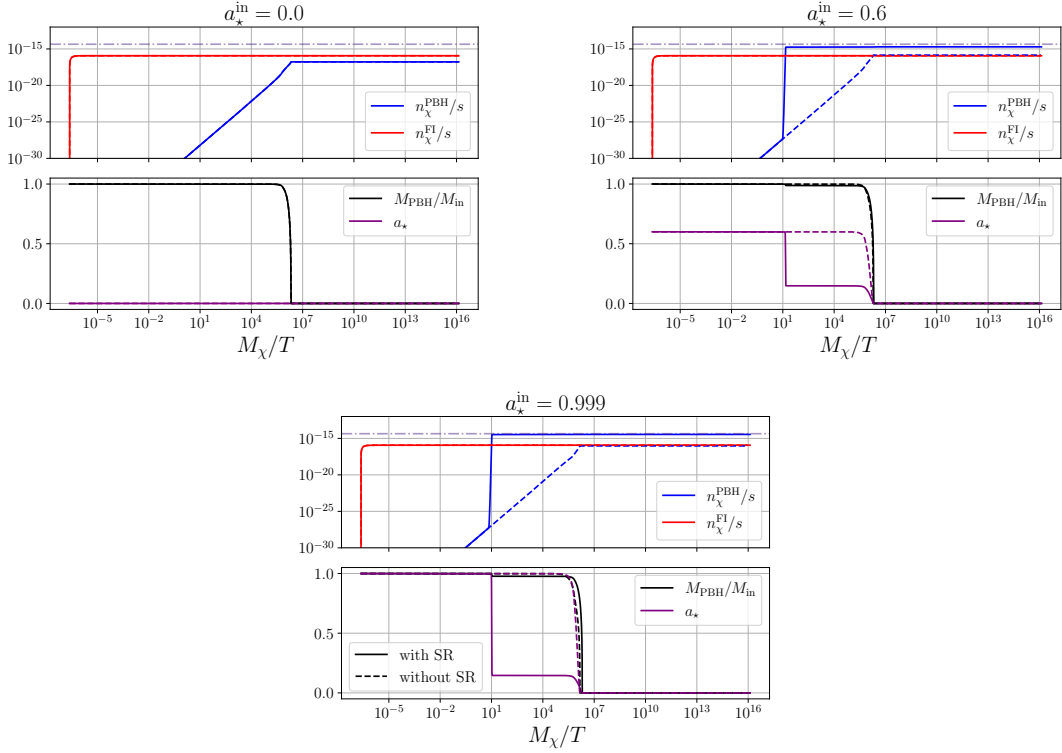


Figure 4. Evolution of DM relic $n_\chi/s(T)$, PBH's mass and PBH's angular momentum as functions of M_χ/T . The blue lines and the red lines represent the DM from PBH and freeze-in, respectively. The black lines and the purple lines represent the evolution of PBH's mass and angular momentum, respectively. The solid lines describe the case taking the superradiance into account and the dashed lines describe the case without superradiance. The gray horizontal lines correspond to the correct DM relic abundance. We set $M_{\text{in}} = 10^8$ g, $\beta = 10^{-20}$ and $M_\chi = 10^5$ GeV.

In the case of pNGB DM produced by Hawking radiation and superradiance, the Boltzmann equations for the PBH-DM system read,

$$Ha \frac{dN_\chi^{\text{SR}}}{da} = \Gamma_{\text{SR}} N_\chi^{\text{SR}}, \quad (4.17)$$

$$Ha \frac{dM_{\text{PBH}}}{da} = -\varepsilon(M_{\text{PBH}}, a_\star) \frac{M_{\text{Pl}}^4}{M_{\text{PBH}}^2} - M_\chi \Gamma_{\text{SR}} N_\chi^{\text{SR}}, \quad (4.18)$$

$$Ha \frac{da_\star}{da} = -a_\star [\gamma(M_{\text{PBH}}, a_\star) - 2\varepsilon(M_{\text{PBH}}, a_\star)] \frac{M_{\text{Pl}}^4}{M_{\text{PBH}}^3} - \left[\sqrt{2} - 2\alpha a_\star \right] \Gamma_{\text{SR}} N_\chi^{\text{SR}} \frac{M_{\text{Pl}}^2}{M_{\text{PBH}}^2}, \quad (4.19)$$

$$Ha \frac{dN_\chi^{\text{PBH}}}{da} = \frac{\varrho_{\text{PBH}}}{M_{\text{PBH}}} [\Gamma_{\text{PBH} \rightarrow \chi} + \Gamma_{\text{SR}} N_\chi^{\text{SR}}], \quad (4.20)$$

and the equations for DM produced by UV freeze-in is,

$$Ha \frac{dN_\chi^{\text{FI}}}{da} = 2a^3 \gamma_{\chi\chi \rightarrow H^\dagger H}. \quad (4.21)$$

N_χ represents the total number of pNGB DM particles produced via superradiance by an individual black hole. The first line describes the number of pNGB DM particles generated through black hole superradiance. The second and third lines illustrate the decay of black hole mass and angular momentum, accounting for both Hawking radiation and superradiance. The fourth formula gives the total number of DM particles produced through Hawking radiation and superradiance. Finally, the UV freeze-in mechanism for generating pNGB DM is included. We solve Eqs. (4.11)-(4.14) and Eqs. (4.17)-(4.21) numerically by using the Python package ULYSSES [67, 77, 78].

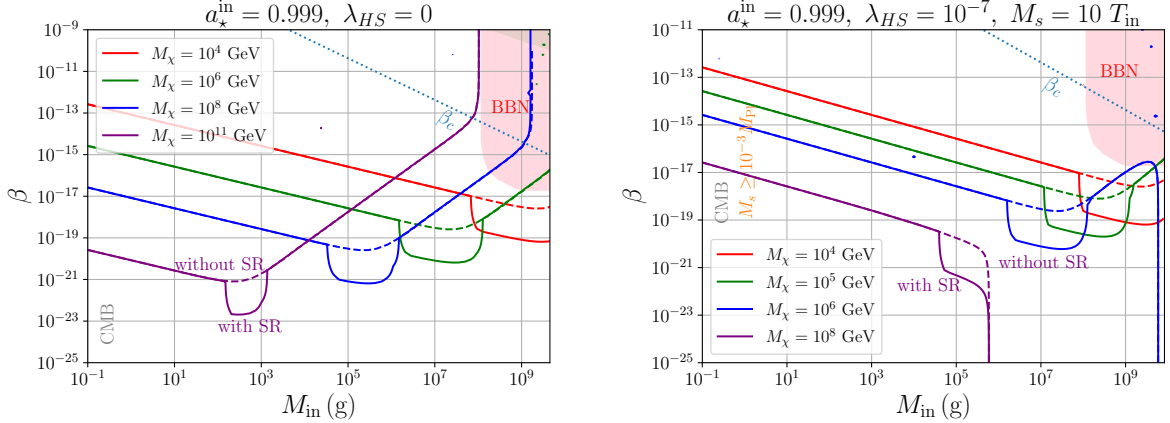


Figure 5. Left panel: Contour plot showing regions where the relic abundance of DM satisfies correct DM relic density $\Omega_{\text{DM}} h^2 = 0.12$, considering contributions from Hawking radiation and superradiance. The “SR” represents the superradiance. The dashed lines represent the cases without superradiance. Right panel: Contour plot showing regions where the relic abundance of DM satisfies $\Omega_{\text{DM}} h^2 = 0.12$, accounting for Hawking radiation, superradiance, and UV freeze-in.

As an example, We set the parameters $M_{\text{in}} = 10^8$ g, $\beta = 10^{-20}$, $M_\chi = 10^5$ GeV and the numerical results are shown in Fig. 4. We show the evolution of DM relic density from PBHs and freeze-in as functions of M_χ/T . And we also show the evolution of the mass and angular momentum of PBHs. The solid and dashed lines represent the cases with and without superradiance, respectively. Then we scan over the parameter space and show the contour plot of correct relic density of DM for different values of DM mass in Fig. 5. The initial angular momentum parameter of PBH is fixed to be $a_\star^{\text{in}} = 0.999$. Compared to the left panel, the right panel includes UV freeze-in with $\lambda_{HS} = 10^{-7}$. It can be seen that the superradiance plays an important role at $\alpha \sim \mathcal{O}(0.1)$. For Kerr black holes with $a_\star^{\text{in}} = 0.999$, the superradiance enhances the DM relic abundance by a factor of $\mathcal{O}(10 - 100)$.

5 Gravitational wave

5.1 Gravitational wave from domain wall

The explicit symmetry-breaking term in the Lagrangian reduces the symmetry of the model to a Z_2 symmetry. Consequently, the breaking of Z_2 symmetry leads to the formation of DWs in the Universe. However, since DWs are inherently stable, their energy density would eventually dominate the Universe, which is clearly not physically acceptable. It is known that quantum gravity does not respect any global symmetries. To address this issue, we may

introduce the following term [79, 80].

$$\Delta V = \frac{1}{\Lambda_{\text{QG}}} (c_1 S^5 + c_2 S^3 H^2 + c_3 S H^4) , \quad (5.1)$$

where Λ_{QG} denotes the scale of QG and the prefactors $c_{1,2,3}$ are some constants. Because we have $v_s \gg v$, the bias term is dominated by the first term and we can absorb the prefactors into Λ_{QG} , then one can write the energy bias after replacing fields with their VEVs

$$\Delta V \simeq \frac{1}{\Lambda_{\text{QG}}} v_s^5 . \quad (5.2)$$

Require the DWs annihilate away before they dominate the Universe, we get the following condition [81]:

$$\Delta V^{1/4} > 2.18 \times 10^4 \text{ GeV} \times C_{\text{ann}}^{1/4} \mathcal{A}^{1/2} \left(\frac{\sigma}{10^{27} \text{ GeV}^3} \right)^{1/2} , \quad (5.3)$$

where $\sigma = \frac{4}{3} \sqrt{\lambda_S} v_s^3$ is the surface tension of the DW, $C_{\text{ann}} \simeq 2$ is a dimensionless constant, and $\mathcal{A} \simeq 0.8 \pm 0.1$ is the area parameter. In terms of the breaking scale, this condition translates to

$$v_s < 1.95 \times 10^{12} \text{ GeV} \left(\frac{10^{30} \text{ GeV}}{\Lambda_{\text{QG}}} \right) \left(\frac{10^{-6}}{\lambda_S} \right) . \quad (5.4)$$

Besides, the DWs could decay into SM particles and destroy the predictions of BBN. In order to avoid this, there is another constraint on the bias energy [81]:

$$\Delta V^{1/4} > 16.03 \text{ GeV} \times C_{\text{ann}}^{1/4} \mathcal{A}^{1/4} \left(\frac{\sigma}{10^{27} \text{ GeV}^3} \right)^{1/4} , \quad (5.5)$$

or equivalently,

$$v_s > 375.32 \text{ GeV} \left(\frac{\lambda_S}{10^{-6}} \right)^{1/4} \left(\frac{\Lambda_{\text{QG}}}{10^{30} \text{ GeV}} \right) , \quad (5.6)$$

under which the DWs can annihilate away before the BBN. After the DWs annihilate, the peak frequency of the resulting GW is given by [81–83]

$$\begin{aligned} f_p^{\text{DW}} &\simeq \\ 3.75 \times 10^{-4} \text{ Hz} & C_{\text{ann}}^{-1/2} \mathcal{A}^{-1/2} \left(\frac{g_*(T_{\text{ann}})}{10} \right)^{1/4} \left(\frac{g_{*s}(T_{\text{ann}})}{10} \right)^{-1/3} \left(\frac{10^{27} \text{ GeV}^3}{\sigma} \right)^{1/2} \left(\frac{\Delta V}{10^{16} \text{ GeV}^4} \right)^{1/2} , \\ &\simeq 2.57 \text{ Hz} \left(\frac{g_*(T_{\text{ann}})}{10} \right)^{1/4} \left(\frac{g_{*s}(T_{\text{ann}})}{10} \right)^{-1/3} \left(\frac{\lambda_S}{10^{-6}} \right)^{-1/4} \left(\frac{v_s}{10^{12} \text{ GeV}} \right) \left(\frac{\Lambda_{\text{QG}}}{10^{30} \text{ GeV}} \right)^{-1/2} , \end{aligned} \quad (5.7)$$

and peak energy density spectrum of DW collapse,

$$\Omega_p^{\text{DW}} h^2 \simeq 5.3 \times 10^{-4} \times \epsilon_{\text{GW}} C_{\text{ann}}^2 \mathcal{A}^4 \left(\frac{g_{*s}(T_{\text{ann}})}{10} \right)^{-4/3} \left(\frac{\sigma}{10^{27} \text{ GeV}^3} \right)^4 \left(\frac{10^{16} \text{ GeV}^4}{\Delta V} \right)^2 , \quad (5.8)$$

where $\epsilon_{\text{GW}} \simeq 0.7$ [84] represents the fraction of energy radiated into GW. We adopt the following power-law spectrum for the DW GW signals [85, 86],

$$\Omega_{\text{GW}}^{\text{DW}} h^2 = \Omega_p^{\text{DW}} h^2 \frac{(a+b)^c}{(bx^{-a/c} + ax^{b/c})^c} , \quad (5.9)$$

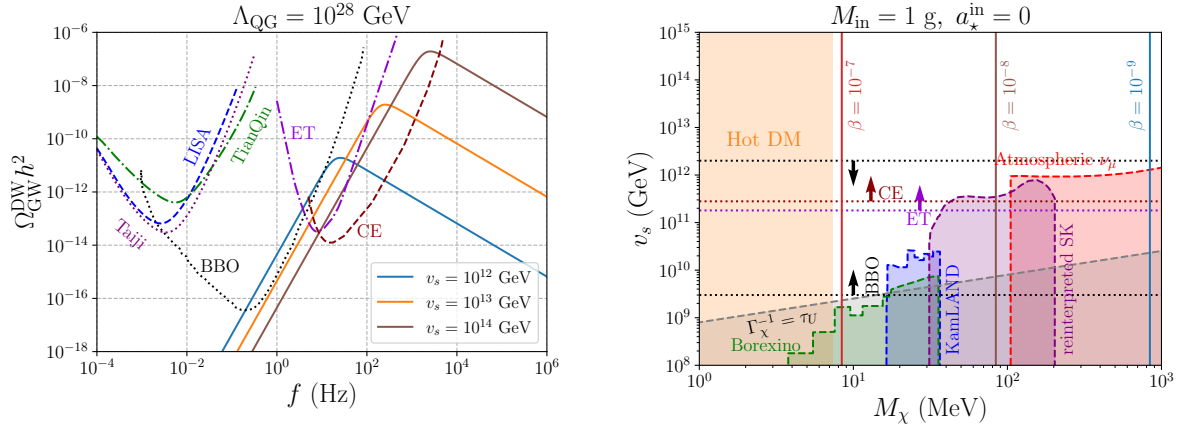


Figure 6. Left panel: The DW GW spectrum for $v_s = 10^{12}$, 10^{13} and 10^{14} GeV and the sensitivity curves of LISA, Tianqin, Taiji, BBO, CE and ET. Right panel: The case of $M_{\text{in}} = 1$ g for Schwarzschild black holes. The region between the two black lines is accessible to BBO experiments assuming $\text{SNR} > 10$, while areas above the dark red and dark purple lines are detectable by CE and ET, respectively. The green, blue, purple and red regions are excluded by Borexino, KamLAND, reinterpreted SK, and atmospheric ν_μ spectra. On the vertical lines the correct DM abundance is fulfilled with the corresponding values of β .

where $x \equiv f/f_p^{\text{DW}}$ and $a = 3$. Numerical simulations suggest that $b \simeq c \simeq 1$ [84].

It has been argued that the successful formation of DWs requires the mass of real scalar M_s has to be smaller than the reheating temperature T_{in} . So the case with PBH and UV freeze-in can not produce detectable DW GWs. However, the DW GWs can detect the pNGB DM produced purely from PBHs instead. For given GW spectrum $\Omega_{\text{GW}} h^2$, to quantify the detectability of the GW signals, we calculate the signal-to-noise ratio [87–89],

$$\text{SNR} = \sqrt{\mathcal{T} \int_{f_{\text{min}}}^{f_{\text{max}}} df \left(\frac{\Omega_{\text{GW}} h^2}{\Omega_{\text{sens}} h^2} \right)^2}, \quad (5.10)$$

where $\Omega_{\text{sens}} h^2$ is the noise spectrum of the experiments and \mathcal{T} is the duration time of the experiment. We assume the GW is detectable when $\text{SNR} > 10$. In the left panel of Fig. 6 we fix $\Lambda_{\text{QG}} = 10^{28}$ GeV and show the DW GWs for $v_s = 10^{12}$, 10^{13} , 10^{14} GeV. The GW signals could be detected by BBO [90, 91], Cosmic Explorer (CE) [92] and Einstein telescope (ET) [93, 94]. If the breaking scale v_s is lower, the signals can also be probed by LISA [95], TianQin [96] and Taiji [97].

Notably, assuming the pNGB is Majoron, the DM can directly decay into the neutrino flux, which is constrained by dedicated experiments such as Borexino [98], KamLAND [99], reinterpreted SK [100], and constraint from atmospheric ν_μ spectra [100]. Here we assume the decay width of pNGB is given by Eq. (2.4). The results are shown in the right panel of Fig. 6. We can see that due to the strong constraints from these experiments, the VEV v_s associated with pNGB DM must be large enough such that the peak frequencies of the corresponding GW signals are higher than 1 Hz. Additionally, although the DW GWs can also help to detect heavy pNGB DM, here we only show the parameter space of the light MeV pNGB. The excluded regions from Borexino, KamLAND, reinterpreted SK and atmospheric ν_μ spectra in the right panel of Fig. 6 are taken from Ref. [59].

By the way, it should be noted that the DW annihilation itself can produce the pNGB and PBHs [101–103] which we leave in our future work.

5.2 Induced gravitational wave

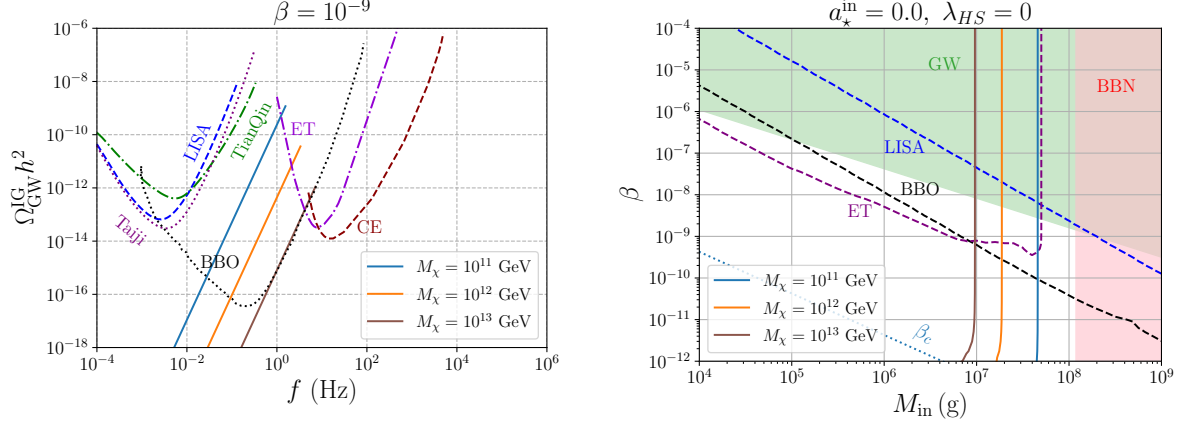


Figure 7. Left panel: Induced GW spectrum for $M_\chi = 10^{11}$, 10^{12} and 10^{13} GeV. Right panel: The contour plot of superheavy DM relic density where the DM mass is $M_\chi = 10^{11}$ GeV, 10^{12} GeV and 10^{13} GeV. We take the Schwarzschild case with $a_\star^{\text{in}} = 0$ and $\lambda_{HS} = 0$. The regions above the black, blue, and purple dashed lines represent areas that can be observed by GW experiments with $\text{SNR} > 10$.

After PBHs form, they distribute randomly throughout the Universe following Poissonian statistics [104]. When the PBHs begin to dominate the energy density of the Universe, this inhomogeneous distribution of PBHs leads to curvature perturbations. Subsequently, at second order, these perturbations can generate GWs. The present-day induced GW spectrum can be written as [70, 105]

$$\Omega_{\text{GW}}^{\text{IG}} h^2 \simeq \Omega_p^{\text{IG}} h^2 \left(\frac{f}{f_p^{\text{IG}}} \right)^{11/3} \Theta(f_p^{\text{IG}} - f) , \quad (5.11)$$

where

$$\Omega_p^{\text{IG}} h^2 \simeq 9 \times 10^{-7} \left(\frac{\beta}{10^{-8}} \right)^{16/3} \left(\frac{M_{\text{in}}}{10^7 \text{ g}} \right)^{34/9} \quad (5.12)$$

indicates the peak amplitude of GW spectrum. The f_p^{IG} in Eq. (5.11) corresponds to the cutoff that is derived from the mean separation between PBHs, below which the PBHs cannot be viewed as continued fluid anymore. The peak frequency is found to be

$$f_p^{\text{IG}} \simeq 1.7 \times 10^3 \text{ Hz} \left(\frac{M_{\text{in}}}{10^4 \text{ g}} \right)^{-5/6} . \quad (5.13)$$

From Eq. (3.24), we can get the relation between the DM mass and the initial PBH mass,

$$M_{\text{in}} = 2.81 \times 10^8 \text{ g} \left(\frac{M_\chi}{10^9 \text{ GeV}} \right)^{-2/5} , \quad (5.14)$$

then we get,

$$f_p^{\text{IG}} \simeq 0.33 \text{ Hz} \left(\frac{M_\chi}{10^9 \text{ GeV}} \right)^{1/3}. \quad (5.15)$$

Therefore, the peak frequency of induced GWs is directly linked to the DM mass, providing a novel approach for detecting DM. We show the results in Fig. 7. The left panel presents the spectrum of induced GWs. The right panel shows the contour plot for superheavy DM, along with the observational regions accessible to the GW experiments, like LISA, BBO, and ET.

5.3 Gravitational waves from primordial black hole evaporation

Even if PBHs never dominate the Universe, they can produce GWs through the direct evaporation of gravitons. The spectrum of these GWs can be expressed as follows:

$$\frac{d\rho_{\text{GW}}}{dt dp} = n_{\text{PBH}}(t) p \frac{dN_{\text{grav}}}{dt dp}. \quad (5.16)$$

By using $n_{\text{PBH}}(t) = n_{\text{PBH}}(t_{\text{in}})(a_{\text{in}}/a)^3$, the GW spectra at t_{evap} can be written as

$$\frac{d\rho_{\text{GW, evap}}}{d\ln p_{\text{evap}}} = \frac{1}{\pi^3} n_{\text{PBH}}(t_{\text{in}}) p_{\text{evap}}^4 \int_{t_{\text{in}}}^{t_{\text{evap}}} dt \left(\frac{a_{\text{in}}}{a} \right)^3 \frac{\sigma_{s_i}^{lm}}{\exp[(p(t) - m\Omega)/T_{\text{PBH}}] - 1}. \quad (5.17)$$

Here, we omit the summation of l and m . By using the relation

$$p(t) = p_{\text{evap}} \frac{a_{\text{evap}}}{a} = p_0 \frac{a_0}{a}, \quad H(t) = H_{\text{in}} \left(\frac{a_{\text{in}}}{a} \right)^2 = \frac{\gamma M_{\text{Pl}}^2}{2M_{\text{in}}} \left(\frac{a_{\text{in}}}{a} \right)^2, \quad (5.18)$$

where p_0 is the momentum of graviton at present. Then we can get the GW energy spectrum at present,

$$\begin{aligned} \frac{d\rho_{\text{GW},0}}{d\ln p_0} &= \frac{1}{\pi^3 H_{\text{in}}} n_{\text{PBH}}(t_{\text{in}}) p_0^3 \frac{a_{\text{in}}}{a_0} \int_{\frac{p_0 a_0}{a_{\text{evap}}}}^{\frac{p_0 a_0}{a_{\text{in}}}} dp \frac{\sigma_{s_i}^{lm}}{\exp[(p - m\Omega)/T_{\text{PBH}}] - 1} \\ &= \frac{1}{\pi^3 H_{\text{in}}} \frac{\beta \rho_r(T_{\text{in}})}{M_{\text{in}}} p_0^4 \frac{a_{\text{in}}}{a_0} \int_{\frac{a_0}{a_{\text{evap}}}}^{\frac{a_0}{a_{\text{in}}}} dx \frac{\sigma_{s_i}^{lm}}{\exp[(xp_0 - m\Omega)/T_{\text{PBH}}] - 1}, \end{aligned} \quad (5.19)$$

where in the second line we define $x = p/p_0$ and use Eq. (3.4). Then we get

$$\frac{d\rho_{\text{GW},0}}{d\ln p_0} = 2 \times 10^{32} \beta M_{\text{in}}^{-3/2} p_0^4 \int_{\frac{a_0}{a_{\text{evap}}}}^{\frac{a_0}{a_{\text{in}}}} dx \frac{\sigma_{s_i}^{lm}}{\exp[(xp_0 - m\Omega)/T_{\text{PBH}}] - 1}, \quad (5.20)$$

with

$$\frac{a_0}{a_{\text{in}}} \simeq \left(\frac{g_{*s}(T_{\text{in}})}{g_{*s}(T_0)} \right)^{1/3} \frac{T_{\text{in}}}{T_0}, \quad \frac{a_0}{a_{\text{evap}}} = \frac{a_0}{a_{\text{in}}} \frac{a_{\text{in}}}{a_{\text{evap}}}. \quad (5.21)$$

Determining the precise value of a_{evap} requires solving the Boltzmann equations of Kerr PBHs numerically, with or without superradiance. We use the public code BlackHawk [106, 107] to get the greybody factors of Hawking radiation, which have the relation with the absorption cross section, $\Gamma(M_{\text{PBH}}, p) \equiv \sigma_{s_i}(M_{\text{PBH}}, p) p^2 / \pi$. The relic abundance of GW from PBH evaporation is

$$\Omega_{\text{GW}}^{\text{BH}} h^2 = \frac{h^2}{\rho_c} \frac{d\rho_{\text{GW},0}}{d\ln p_0}. \quad (5.22)$$

	M_χ (GeV)	M_{in} (g)	a_\star^{in}	β
BP_1 (without SR)	10^5	10^8	0.999	4.7×10^{-19}
BP_2 (with SR)	10^5	10^8	0.999	1.3×10^{-20}

Table 1. Two sets of parameters that satisfy the DM relic abundance with and without considering the superradiance.

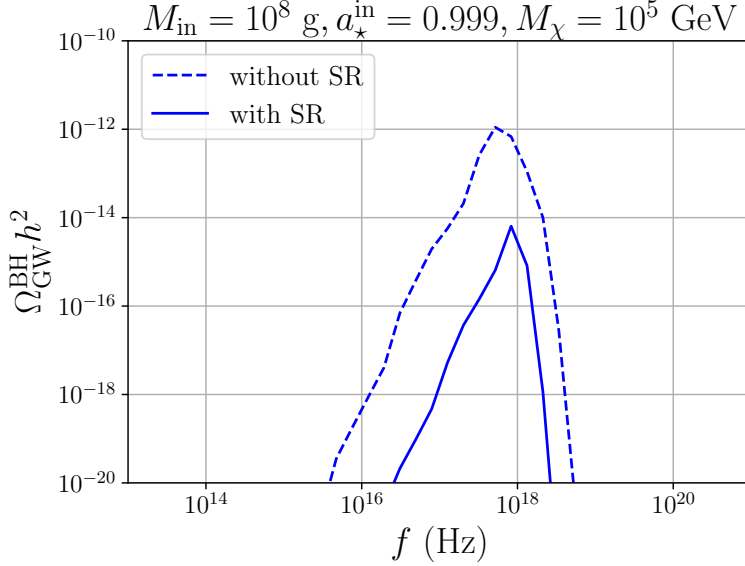


Figure 8. GW spectra generated by Hawking radiation. The solid and dashed lines correspond to the case with and without superradiance, respectively.

The result of GW spectra are shown in Fig. 8. The benchmark parameters are listed in Tab. 1 where we set the same values of M_χ , M_{in} and a_\star^{in} . We can see that the effect of superradiance significantly alters the GW spectrum generated by Hawking radiation. This is because the superradiance process modifies the evolution of Kerr black holes in terms of their mass and angular momentum. Due to the appearance of superradiation, a large amount of energy and angular momentum is carried away by DM, so the strength of GW from Hawking radiation is significantly reduced. Although such extremely high-frequency GW spectra cannot yet be observed by current detectors, they may be detectable in the future, enabling us to effectively distinguish the contribution of superradiance.

6 Possible interpretation of the KM3-230213A neutrino event from pNGB decay

Recently, the KM3NeT collaboration has reported the detection of a high energy neutrino event, with an energy of 220_{-100}^{+570} PeV [108]. This ultra-high energetic neutrino signals may point towards some astrophysical interpretations [109] or cosmic origin [110–113]. In this work, we consider the origin of this neutrino event from pNGB decay.

We use the models in Refs. [12, 13], which introduce the gauged $U(1)_{B-L}$ symmetry. The S carries a charge of $Q_{B-L} = +1$. Additionally, we introduce a complex scalar field

$\Phi = (v_\phi + \phi)e^{i\eta}/\sqrt{2}$ with $Q_{B-L} = +2$. The potential of the UV model enlarges Eq. (2.1) as,

$$V(H, S, \Phi) = -\frac{\mu_H^2}{2}|H|^2 - \frac{\mu_S^2}{2}|S|^2 - \frac{\mu_\Phi^2}{2}|\Phi|^2 + \frac{\lambda_H}{2}|H|^4 + \frac{\lambda_S}{2}|S|^4 + \frac{\lambda_\Phi}{2}|\Phi|^4, \quad (6.1)$$

$$+ \lambda_{HS}|H|^2|S|^2 + \lambda_{H\Phi}|H|^2|\Phi|^2 + \lambda_{S\Phi}|S|^2|\Phi|^2 - \left(\frac{\mu_c}{\sqrt{2}}\Phi^* S^2 + \text{h.c.} \right).$$

We set $\lambda_{H\Phi} = \lambda_{S\Phi} = 0$ for simplicity. Due to the last term, after the symmetry breaking of Φ we can get the explicit breaking term in Eq. (2.1). The Φ can couple to the right-handed neutrinos through the term $f\Phi\bar{\nu}_R^c\nu_R$. The symmetry breaking of Φ gives the right-handed neutrino a mass of $M_N = f v_\phi/\sqrt{2}$. Additionally, the electroweak symmetry breaking of the SM Higgs field H provides a Dirac mass for neutrinos, $m_D = y^\nu v/\sqrt{2}$. Thus, based on the standard type-I seesaw mechanism, the neutrino mass is given by $(m_\nu)_{\alpha\beta} \approx (m_D M_N^{-1} m_D^T)_{\alpha\beta}$. Due to the final mixing term, χ and η can mix with each other, with the mixing angle being proportional to v_s/v_ϕ . One of the NGBs is absorbed by the dark gauge boson Z' , while the other remains as a physical pNGB. The pNGB can decay into neutrinos through NGB mixing and active-sterile neutrino mixing. When $v_s/v_\phi \ll 1$, this decay width is much smaller than that of the Majoron, which is given by Eq. (2.4). Additionally, because we only consider the case $M_\chi < M_s$, the pNGB can decay into SM fermions through the off-shell s and Z' , $\chi \rightarrow sZ' \rightarrow \bar{f}_{\text{SM}} f_{\text{SM}} \bar{f}_{\text{SM}} f_{\text{SM}}$ [13]. The decay width is proportional to M_χ^5 and $\sin^2 \theta_{sh}^2$ where $\sin \theta_{sh}$ is the mixing between the s and the SM Higgs. Therefore this decay channel may dominate when M_χ is large and the mixing angle is non-zero. Note that the mixing angle also serve as the origin of freeze-in production of pNGB DM. We neglect the kinetic mixing of the gauge bosons in this analysis.

In order to explain the high-energy neutrino event, we set $M_\chi = 440$ PeV. For such superheavy DM, traditional production mechanism like freeze-out is hard to work. However, in this work we have shown that the DM could be directly produced by black holes. We only include the decay channels of pNGB DM into neutrinos by setting $\sin \theta_{sh} = 0$ for which the pNGB DM is purely produced by PBH evaporation, and consider their secondaries such as gamma-rays and high energy neutrinos which could explain the event of KM3NeT. The neutrino flux can be estimated as

$$\frac{d^2 \Phi_\nu^G}{dE_\nu d\Omega} = \frac{1}{\tau_\chi} \frac{\mathcal{D}}{4\pi M_\chi} \frac{dN_\nu}{dE_\nu}, \quad (6.2)$$

where dN_ν/dE_ν is the neutrino energy spectrum and the \mathcal{D} -factor is defined as

$$\mathcal{D} = \frac{1}{\Delta\Omega} \int_{\Delta\Omega} d\Omega \int_0^{s_{\text{max}}} ds \rho(r(s, \psi)), \quad (6.3)$$

where $r(s, \psi) = \sqrt{s^2 + r_\odot^2 - 2sr_\odot \cos \psi}$ is the radial coordinate, $\cos \psi = \cos b \cos l$ with (b, l) being the galactic coordinates, $d\Omega = d\sin b dl$ and $\Delta\Omega = \int_l \int_b d\Omega$, $r_\odot \simeq 8.5$ kpc is the distance from the center of the Milky Way to the solar system. And $s_{\text{max}} = \sqrt{d_{\text{MW}}^2 - r_\odot^2 \sin^2 \psi} + r_\odot \cos \psi$, where $d_{\text{MW}} = 40$ kpc is the diameter of the Milky Way. The DM density profile $\rho(r)$ in the Milky Way can be given as

$$\rho(r) = \frac{\rho_c}{\left(\frac{r}{r_s}\right)^\gamma \left[1 + \left(\frac{r}{r_s}\right)^\alpha\right]^{(\beta-\gamma)/\alpha}}, \quad (6.4)$$

where r_s is the scale radius and α, β , and γ are slope parameters. For the Navarro-Frenk-White (NFW) profile [114, 115] $\alpha = 1$, $\beta = 3$, $\gamma = 1$, $r_s = 20$ kpc, and we set ρ_c such that $\rho(r_\odot) = 0.4 \text{ GeV cm}^{-3}$. We compute the neutrino flux for the inner Galactic plane, $15^\circ < l < 125^\circ$, $-5^\circ < b < 5^\circ$.

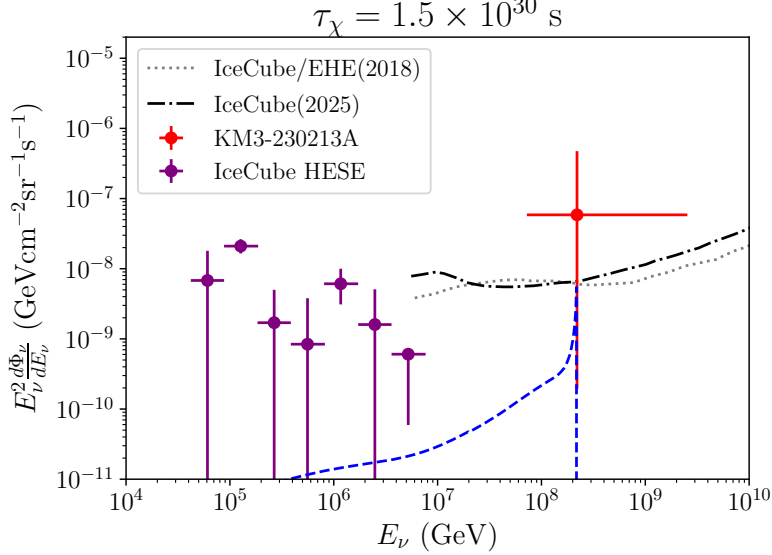


Figure 9. Neutrino flux (the blue dashed line) from pNGB DM decay. The red data point shows the high-energy neutrino event. The purple data points show the IceCube’s HESE events. The gray dotted line and the black dashed dotted line correspond to IceCube-EHE data and 12.6 years of IceCube data, respectively.

The extragalactic neutrino flux resulting from the decay of pNGB DM is [116]

$$\frac{d\Phi_\nu^{\text{EG}}}{dE_\nu} = \frac{1}{\tau_\chi} \frac{1}{4\pi M_\chi} \int_0^\infty dz \frac{\rho_0 c/H_0}{\sqrt{\Omega_m(1+z)^3 + \Omega_\Lambda}} \frac{1}{1+z} \left(\frac{dN_\nu}{dE'_\nu} \right)_{E'_\nu=(1+z)E_\nu}, \quad (6.5)$$

where z is the redshift and $\rho_0 = 1.15 \times 10^{-6} \text{ GeV cm}^{-3}$ is the present cosmological average DM density. $\Omega_m = 0.315$ and $\Omega_\Lambda = 0.685$ [71] are the energy fraction of matter and vacuum energy, respectively. $c/H_0 = 1.37 \times 10^{28} \text{ cm}$ is the proper Hubble radius. Then the total flux per unit solid angle is

$$\frac{d\Phi_\nu}{dE_\nu} \equiv \frac{d^2\Phi_\nu^{\text{G}}}{dE_\nu d\Omega} + \frac{1}{4\pi} \frac{d\Phi_\nu^{\text{EG}}}{dE_\nu} \quad (6.6)$$

We obtain the neutrino spectrum dN_ν/dE_ν by using the publicly available code HDMSpectra [117]. We take the life time of DM τ_χ as a free parameter. Also it is assumed that due to the neutrino oscillations, the neutrinos have the flavor ratio 1:1:1 when reaching the Earth.

The non-observation of the high-energy neutrino event by experiments like IceCube sets the upper limit on the high-energy neutrino flux. The predicted neutrino flux is shown in terms of the blue dashed line in Fig. 9. It can be seen that the flux fits the observation of KM3NeT well. The purple data points show the IceCube’s HESE events [118]. The gray dotted line and the black dashed dotted line correspond to IceCube-EHE data [119] and 12.6 years of IceCube data [120], respectively. The lifetime of DM must exceed $1.5 \times 10^{30} \text{ s}$

to remain consistent with IceCube constraints. This also tells us why the Majoron cannot account for this high-energy signal. The Majoron's lifetime is not sufficiently long for $v_s \lesssim M_{\text{Pl}}$.

7 Conclusions and discussions

Due to the nature of NGB, the pNGB DM as a compelling DM candidate, is unlikely to be produced via the traditional thermal freeze-out mechanism and is instead more plausibly generated through alternative non-thermal processes. Thus, in this work, we have explored novel production mechanisms for pNGB DM via Hawking radiation and superradiance from PBHs, as well as the associated GW signatures.

Our study encompasses the production of both light and superheavy pNGB DM under the influence of Schwarzschild and Kerr black hole scenarios. For Schwarzschild black holes, we derived analytical approximate solutions for the DM production. We investigate the effects of Hawking radiation and UV freeze-in, respectively. In the case of Kerr black holes, we numerically solved the evolution differential equations to determine the DM relic abundance generated by Hawking radiation and superradiance.

Additionally, we explored the GW signals linked to these processes, identifying detectable signatures from DW annihilation and the induced GWs, which are within the sensitivities of experiments such as LISA, TianQin, Taiji, BBO, ET, CE, and other proposals. Furthermore, high-frequency GWs resulting from PBH evaporation may be accessible to future high-frequency GW detection experiments.

Finally, we proposed that in a viable UV completion model, the pNGB decay could account for the recently reported $\mathcal{O}(100)$ PeV neutrino event KM3-230213A at KM3NeT. The pNGB decays through the scalar mixing and is long-lived enough to avoid the constraint from the experiments like IceCube.

These findings highlight the interplay between black hole physics, DM production, and multi-messenger signals, emphasizing the relevance of forthcoming experimental advancements in probing the fundamental nature of DM.

Acknowledgments

We thank Yuber F. Perez-Gonzalez and Andrew Cheek for the helpful guidance about their code ULYSSES. This work is supported by the National Natural Science Foundation of China (NNSFC) under Grant No.12205387 and No.12475111.

References

- [1] SUPERCDMS collaboration, *New Results from the Search for Low-Mass Weakly Interacting Massive Particles with the CDMS Low Ionization Threshold Experiment*, *Phys. Rev. Lett.* **116** (2016) 071301 [[1509.02448](#)].
- [2] LUX collaboration, *Results from a search for dark matter in the complete LUX exposure*, *Phys. Rev. Lett.* **118** (2017) 021303 [[1608.07648](#)].
- [3] PANDAX-II collaboration, *Dark Matter Results from First 98.7 Days of Data from the PandaX-II Experiment*, *Phys. Rev. Lett.* **117** (2016) 121303 [[1607.07400](#)].
- [4] CRESST collaboration, *Results on light dark matter particles with a low-threshold CRESST-II detector*, *Eur. Phys. J. C* **76** (2016) 25 [[1509.01515](#)].

- [5] PICO collaboration, *Dark Matter Search Results from the PICO-60 C₃F₈ Bubble Chamber*, *Phys. Rev. Lett.* **118** (2017) 251301 [[1702.07666](#)].
- [6] C. Gross, O. Lebedev and T. Toma, *Cancellation Mechanism for Dark-Matter–Nucleon Interaction*, *Phys. Rev. Lett.* **119** (2017) 191801 [[1708.02253](#)].
- [7] D. Azevedo, M. Duch, B. Grzadkowski, D. Huang, M. Iglicki and R. Santos, *One-loop contribution to dark-matter-nucleon scattering in the pseudo-scalar dark matter model*, *JHEP* **01** (2019) 138 [[1810.06105](#)].
- [8] K. Ishiwata and T. Toma, *Probing pseudo Nambu-Goldstone boson dark matter at loop level*, *JHEP* **12** (2018) 089 [[1810.08139](#)].
- [9] K. Huitu, N. Koivunen, O. Lebedev, S. Mondal and T. Toma, *Probing pseudo-Goldstone dark matter at the LHC*, *Phys. Rev. D* **100** (2019) 015009 [[1812.05952](#)].
- [10] C. Arina, A. Beniwal, C. Degrande, J. Heisig and A. Scaffidi, *Global fit of pseudo-Nambu-Goldstone Dark Matter*, *JHEP* **04** (2020) 015 [[1912.04008](#)].
- [11] I.Z. Rothstein, K.S. Babu and D. Seckel, *Planck scale symmetry breaking and majoron physics*, *Nucl. Phys. B* **403** (1993) 725 [[hep-ph/9301213](#)].
- [12] Y. Abe, T. Toma and K. Tsumura, *Pseudo-Nambu-Goldstone dark matter from gauged $U(1)_{B-L}$ symmetry*, *JHEP* **05** (2020) 057 [[2001.03954](#)].
- [13] N. Okada, D. Raut and Q. Shafi, *Pseudo-Goldstone dark matter in a gauged $B - L$ extended standard model*, *Phys. Rev. D* **103** (2021) 055024 [[2001.05910](#)].
- [14] R.N. Mohapatra and N. Okada, *Conformal B - L and pseudo-Goldstone dark matter*, *Phys. Rev. D* **107** (2023) 095023 [[2302.11072](#)].
- [15] D.-Y. Liu, C. Cai, X.-M. Jiang, Z.-H. Yu and H.-H. Zhang, *Ultraviolet completion of pseudo-Nambu-Goldstone dark matter with a hidden $U(1)$ gauge symmetry*, *JHEP* **02** (2023) 104 [[2208.06653](#)].
- [16] W. Chao, M. Jin, H.-J. Li, Y.-Q. Peng and Y. Wang, *Axionlike dark matter from the type-II seesaw mechanism*, *Phys. Rev. D* **109** (2024) 115027 [[2210.13233](#)].
- [17] M. Frigerio, T. Hambye and E. Masso, *Sub-GeV dark matter as pseudo-Goldstone from the seesaw scale*, *Phys. Rev. X* **1** (2011) 021026 [[1107.4564](#)].
- [18] L.J. Hall, K. Jedamzik, J. March-Russell and S.M. West, *Freeze-In Production of FIMP Dark Matter*, *JHEP* **03** (2010) 080 [[0911.1120](#)].
- [19] R. Allahverdi, J. Dent and J. Osinski, *Nonthermal production of dark matter from primordial black holes*, *Phys. Rev. D* **97** (2018) 055013 [[1711.10511](#)].
- [20] O. Lennon, J. March-Russell, R. Petrossian-Byrne and H. Tillim, *Black Hole Genesis of Dark Matter*, *JCAP* **04** (2018) 009 [[1712.07664](#)].
- [21] S.M. Boucenna, F. Kuhnel, T. Ohlsson and L. Visinelli, *Novel Constraints on Mixed Dark-Matter Scenarios of Primordial Black Holes and WIMPs*, *JCAP* **07** (2018) 003 [[1712.06383](#)].
- [22] L. Morrison, S. Profumo and Y. Yu, *Melanopogenesis: Dark Matter of (almost) any Mass and Baryonic Matter from the Evaporation of Primordial Black Holes weighing a Ton (or less)*, *JCAP* **05** (2019) 005 [[1812.10606](#)].
- [23] D. Hooper, G. Krnjaic and S.D. McDermott, *Dark Radiation and Superheavy Dark Matter from Black Hole Domination*, *JHEP* **08** (2019) 001 [[1905.01301](#)].
- [24] J. Adamek, C.T. Byrnes, M. Gosenca and S. Hotchkiss, *WIMPs and stellar-mass primordial black holes are incompatible*, *Phys. Rev. D* **100** (2019) 023506 [[1901.08528](#)].

- [25] P. Gondolo, P. Sandick and B. Shams Es Haghi, *Effects of primordial black holes on dark matter models*, *Phys. Rev. D* **102** (2020) 095018 [[2009.02424](#)].
- [26] A. Chaudhuri and A. Dolgov, *PBH Evaporation, Baryon Asymmetry, and Dark Matter*, *J. Exp. Theor. Phys.* **133** (2021) 552 [[2001.11219](#)].
- [27] I. Masina, *Dark matter and dark radiation from evaporating primordial black holes*, *Eur. Phys. J. Plus* **135** (2020) 552 [[2004.04740](#)].
- [28] I. Baldes, Q. Decant, D.C. Hooper and L. Lopez-Honorez, *Non-Cold Dark Matter from Primordial Black Hole Evaporation*, *JCAP* **08** (2020) 045 [[2004.14773](#)].
- [29] N. Bernal and O. Zapata, *Self-interacting Dark Matter from Primordial Black Holes*, *JCAP* **03** (2021) 007 [[2010.09725](#)].
- [30] N. Bernal and O. Zapata, *Dark Matter in the Time of Primordial Black Holes*, *JCAP* **03** (2021) 015 [[2011.12306](#)].
- [31] N. Bernal, Y.F. Perez-Gonzalez, Y. Xu and O. Zapata, *ALP dark matter in a primordial black hole dominated universe*, *Phys. Rev. D* **104** (2021) 123536 [[2110.04312](#)].
- [32] N. Bernal, F. Hajkarim and Y. Xu, *Axion Dark Matter in the Time of Primordial Black Holes*, *Phys. Rev. D* **104** (2021) 075007 [[2107.13575](#)].
- [33] B. Barman, D. Borah, S.J. Das and R. Roshan, *Non-thermal origin of asymmetric dark matter from inflaton and primordial black holes*, *JCAP* **03** (2022) 031 [[2111.08034](#)].
- [34] R. Samanta and F.R. Urban, *Testing super heavy dark matter from primordial black holes with gravitational waves*, *JCAP* **06** (2022) 017 [[2112.04836](#)].
- [35] M. Chen, G.B. Gelmini, P. Lu and V. Takhistov, *Primordial black hole neutrinogenesis of sterile neutrino dark matter*, *Phys. Lett. B* **852** (2024) 138609 [[2309.12258](#)].
- [36] T. Kim, P. Lu, D. Marfatia and V. Takhistov, *Regurgitated dark matter*, *Phys. Rev. D* **110** (2024) L051702 [[2309.05703](#)].
- [37] C.J. Shallue, J.B. Muñoz and G.Z. Krnjaic, *Warm Hawking relics from primordial black hole domination*, *JCAP* **02** (2025) 026 [[2406.08535](#)].
- [38] D. Baumann, P.J. Steinhardt and N. Turok, *Primordial Black Hole Baryogenesis*, [hep-th/0703250](#).
- [39] A. Hook, *Baryogenesis from Hawking Radiation*, *Phys. Rev. D* **90** (2014) 083535 [[1404.0113](#)].
- [40] T. Fujita, M. Kawasaki, K. Harigaya and R. Matsuda, *Baryon asymmetry, dark matter, and density perturbation from primordial black holes*, *Phys. Rev. D* **89** (2014) 103501 [[1401.1909](#)].
- [41] D. Hooper and G. Krnjaic, *GUT Baryogenesis With Primordial Black Holes*, *Phys. Rev. D* **103** (2021) 043504 [[2010.01134](#)].
- [42] Y.F. Perez-Gonzalez and J. Turner, *Assessing the tension between a black hole dominated early universe and leptogenesis*, *Phys. Rev. D* **104** (2021) 103021 [[2010.03565](#)].
- [43] S. Datta, A. Ghosal and R. Samanta, *Baryogenesis from ultralight primordial black holes and strong gravitational waves from cosmic strings*, *JCAP* **08** (2021) 021 [[2012.14981](#)].
- [44] N. Bernal, C.S. Fong, Y.F. Perez-Gonzalez and J. Turner, *Rescuing high-scale leptogenesis using primordial black holes*, *Phys. Rev. D* **106** (2022) 035019 [[2203.08823](#)].
- [45] A. Ambrosone, R. Calabrese, D.F.G. Fiorillo, G. Miele and S. Morisi, *Towards baryogenesis via absorption from primordial black holes*, *Phys. Rev. D* **105** (2022) 045001 [[2106.11980](#)].
- [46] M.R. Haque, S. Maity, D. Maity and Y. Mambrini, *Quantum effects on the evaporation of PBHs: contributions to dark matter*, *JCAP* **07** (2024) 002 [[2404.16815](#)].

- [47] B. Barman, M.R. Haque and O. Zapata, *Gravitational wave signatures of cogenesis from a burdened PBH*, *JCAP* **09** (2024) 020 [[2405.15858](#)].
- [48] D. Borah and N. Das, *Successful cogenesis of baryon and dark matter from memory-burdened PBH*, *JCAP* **02** (2025) 031 [[2410.16403](#)].
- [49] B. Barman, K. Loho and O. Zapata, *Asymmetries from a charged memory-burdened PBH*, *JCAP* **02** (2025) 052 [[2412.13254](#)].
- [50] N. Bhaumik, M.R. Haque, R.K. Jain and M. Lewicki, *Memory burden effect mimics reheating signatures on SGWB from ultra-low mass PBH domination*, *JHEP* **10** (2024) 142 [[2409.04436](#)].
- [51] B. Barman, K. Loho and O. Zapata, *Constraining burdened PBHs with gravitational waves*, *JCAP* **10** (2024) 065 [[2409.05953](#)].
- [52] N.P.D. Loc, *Gravitational waves from burdened primordial black holes dark matter*, *Phys. Rev. D* **111** (2025) 023509 [[2410.17544](#)].
- [53] N. Bernal, Y.F. Perez-Gonzalez and Y. Xu, *Superradiant production of heavy dark matter from primordial black holes*, *Phys. Rev. D* **106** (2022) 015020 [[2205.11522](#)].
- [54] A. Ghoshal, Y.F. Perez-Gonzalez and J. Turner, *Superradiant leptogenesis*, *JHEP* **02** (2024) 113 [[2312.06768](#)].
- [55] M. Manno and D. Montanino, *ALPs production from Light Primordial Black Holes: the role of Superradiance*, [2501.14589](#).
- [56] P. Athron, M. Chianese, S. Datta, R. Samanta and N. Saviano, *Impact of memory-burdened black holes on primordial gravitational waves in light of Pulsar Timing Array*, [2411.19286](#).
- [57] S.K. Manna and A. Sil, *Majorons revisited: Light dark matter as a FIMP*, *Phys. Rev. D* **108** (2023) 075026 [[2212.08404](#)].
- [58] P.F. de Salas, D.V. Forero, S. Gariazzo, P. Martínez-Miravé, O. Mena, C.A. Ternes et al., *2020 global reassessment of the neutrino oscillation picture*, *JHEP* **02** (2021) 071 [[2006.11237](#)].
- [59] C. Garcia-Cely and J. Heeck, *Neutrino Lines from Majoron Dark Matter*, *JHEP* **05** (2017) 102 [[1701.07209](#)].
- [60] ICECUBE collaboration, *Search for neutrinos from decaying dark matter with IceCube*, *Eur. Phys. J. C* **78** (2018) 831 [[1804.03848](#)].
- [61] Y. Abe, Y. Hamada, T. Ohata, K. Suzuki and K. Yoshioka, *TeV-scale Majorogenesis*, *JHEP* **07** (2020) 105 [[2004.00599](#)].
- [62] Y. Abe, T. Toma and K. Yoshioka, *Non-thermal Production of PNGB Dark Matter and Inflation*, *JHEP* **03** (2021) 130 [[2012.10286](#)].
- [63] B.J. Carr, K. Kohri, Y. Sendouda and J. Yokoyama, *New cosmological constraints on primordial black holes*, *Phys. Rev. D* **81** (2010) 104019 [[0912.5297](#)].
- [64] B.J. Carr, *The Primordial black hole mass spectrum*, *Astrophys. J.* **201** (1975) 1.
- [65] PLANCK collaboration, *Planck 2018 results. X. Constraints on inflation*, *Astron. Astrophys.* **641** (2020) A10 [[1807.06211](#)].
- [66] BICEP, KECK collaboration, *Improved Constraints on Primordial Gravitational Waves using Planck, WMAP, and BICEP/Keck Observations through the 2018 Observing Season*, *Phys. Rev. Lett.* **127** (2021) 151301 [[2110.00483](#)].
- [67] A. Cheek, L. Heurtier, Y.F. Perez-Gonzalez and J. Turner, *Primordial black hole evaporation and dark matter production. I. Solely Hawking radiation*, *Phys. Rev. D* **105** (2022) 015022 [[2107.00013](#)].

- [68] D.N. Page, *Particle Emission Rates from a Black Hole: Massless Particles from an Uncharged, Nonrotating Hole*, *Phys. Rev. D* **13** (1976) 198.
- [69] J.H. MacGibbon and B.R. Webber, *Quark and gluon jet emission from primordial black holes: The instantaneous spectra*, *Phys. Rev. D* **41** (1990) 3052.
- [70] G. Domènech, C. Lin and M. Sasaki, *Gravitational wave constraints on the primordial black hole dominated early universe*, *JCAP* **04** (2021) 062 [[2012.08151](#)].
- [71] PLANCK collaboration, *Planck 2018 results. VI. Cosmological parameters*, *Astron. Astrophys.* **641** (2020) A6 [[1807.06209](#)].
- [72] A. Boccia, F. Iocco and L. Visinelli, *Constraining the primordial black hole abundance through big-bang nucleosynthesis*, *Phys. Rev. D* **111** (2025) 063508 [[2405.18493](#)].
- [73] S.L. Detweiler, *KLEIN-GORDON EQUATION AND ROTATING BLACK HOLES*, *Phys. Rev. D* **22** (1980) 2323.
- [74] C. Lunardini and Y.F. Perez-Gonzalez, *Dirac and Majorana neutrino signatures of primordial black holes*, *JCAP* **08** (2020) 014 [[1910.07864](#)].
- [75] N. Bernal and F. Hajkarim, *Primordial Gravitational Waves in Nonstandard Cosmologies*, *Phys. Rev. D* **100** (2019) 063502 [[1905.10410](#)].
- [76] P. Arias, N. Bernal, A. Herrera and C. Maldonado, *Reconstructing Non-standard Cosmologies with Dark Matter*, *JCAP* **10** (2019) 047 [[1906.04183](#)].
- [77] A. Granelli, K. Moffat, Y.F. Perez-Gonzalez, H. Schulz and J. Turner, *ULYSSES: Universal LeptogeneSiS Equation Solver*, *Comput. Phys. Commun.* **262** (2021) 107813 [[2007.09150](#)].
- [78] A. Granelli, C. Leslie, Y.F. Perez-Gonzalez, H. Schulz, B. Shuve, J. Turner et al., *ULYSSES, universal LeptogeneSiS equation solver: Version 2*, *Comput. Phys. Commun.* **291** (2023) 108834 [[2301.05722](#)].
- [79] B. Rai and G. Senjanovic, *Gravity and domain wall problem*, *Phys. Rev. D* **49** (1994) 2729 [[hep-ph/9301240](#)].
- [80] D. Borah, N. Das and R. Roshan, *Observable gravitational waves and ΔN_{eff} with global lepton number symmetry and dark matter*, *Phys. Rev. D* **110** (2024) 075042 [[2406.04404](#)].
- [81] K. Saikawa, *A review of gravitational waves from cosmic domain walls*, *Universe* **3** (2017) 40 [[1703.02576](#)].
- [82] N. Chen, T. Li and Y. Wu, *The gravitational waves from the collapsing domain walls in the complex singlet model*, *JHEP* **08** (2020) 117 [[2004.10148](#)].
- [83] S. Bhattacharya, N. Mondal, R. Roshan and D. Vatsyayan, *Leptogenesis, dark matter and gravitational waves from discrete symmetry breaking*, *JCAP* **06** (2024) 029 [[2312.15053](#)].
- [84] T. Hiramatsu, M. Kawasaki and K. Saikawa, *On the estimation of gravitational wave spectrum from cosmic domain walls*, *JCAP* **02** (2014) 031 [[1309.5001](#)].
- [85] C. Caprini et al., *Detecting gravitational waves from cosmological phase transitions with LISA: an update*, *JCAP* **03** (2020) 024 [[1910.13125](#)].
- [86] NANOGrav collaboration, *The NANOGrav 15 yr Data Set: Search for Signals from New Physics*, *Astrophys. J. Lett.* **951** (2023) L11 [[2306.16219](#)].
- [87] C.J. Moore, R.H. Cole and C.P.L. Berry, *Gravitational-wave sensitivity curves*, *Class. Quant. Grav.* **32** (2015) 015014 [[1408.0740](#)].
- [88] M. Breitbach, J. Kopp, E. Madge, T. Opferkuch and P. Schwaller, *Dark, Cold, and Noisy: Constraining Secluded Hidden Sectors with Gravitational Waves*, *JCAP* **07** (2019) 007 [[1811.11175](#)].

- [89] A. Azatov, D. Barducci and F. Sgarlata, *Gravitational traces of broken gauge symmetries*, *JCAP* **07** (2020) 027 [[1910.01124](#)].
- [90] J. Crowder and N.J. Cornish, *Beyond LISA: Exploring future gravitational wave missions*, *Phys. Rev. D* **72** (2005) 083005 [[gr-qc/0506015](#)].
- [91] V. Corbin and N.J. Cornish, *Detecting the cosmic gravitational wave background with the big bang observer*, *Class. Quant. Grav.* **23** (2006) 2435 [[gr-qc/0512039](#)].
- [92] D. Reitze et al., *Cosmic Explorer: The U.S. Contribution to Gravitational-Wave Astronomy beyond LIGO*, *Bull. Am. Astron. Soc.* **51** (2019) 035 [[1907.04833](#)].
- [93] B. Sathyaprakash et al., *Scientific Objectives of Einstein Telescope*, *Class. Quant. Grav.* **29** (2012) 124013 [[1206.0331](#)].
- [94] ET collaboration, *Science Case for the Einstein Telescope*, *JCAP* **03** (2020) 050 [[1912.02622](#)].
- [95] LISA collaboration, *Laser Interferometer Space Antenna*, [1702.00786](#).
- [96] TIANQIN collaboration, *TianQin: a space-borne gravitational wave detector*, *Class. Quant. Grav.* **33** (2016) 035010 [[1512.02076](#)].
- [97] W.-R. Hu and Y.-L. Wu, *The Taiji Program in Space for gravitational wave physics and the nature of gravity*, *Natl. Sci. Rev.* **4** (2017) 685.
- [98] BOREXINO collaboration, *Study of solar and other unknown anti-neutrino fluxes with Borexino at LNGS*, *Phys. Lett. B* **696** (2011) 191 [[1010.0029](#)].
- [99] KAMLAND collaboration, *A study of extraterrestrial antineutrino sources with the KamLAND detector*, *Astrophys. J.* **745** (2012) 193 [[1105.3516](#)].
- [100] S. Palomares-Ruiz, *Model-independent bound on the dark matter lifetime*, *Phys. Lett. B* **665** (2008) 50 [[0712.1937](#)].
- [101] J. Garriga, A. Vilenkin and J. Zhang, *Black holes and the multiverse*, *JCAP* **02** (2016) 064 [[1512.01819](#)].
- [102] H. Deng, J. Garriga and A. Vilenkin, *Primordial black hole and wormhole formation by domain walls*, *JCAP* **04** (2017) 050 [[1612.03753](#)].
- [103] G.B. Gelmini, J. Hyman, A. Simpson and E. Vitagliano, *Primordial black hole dark matter from catastogenesis with unstable pseudo-Goldstone bosons*, *JCAP* **06** (2023) 055 [[2303.14107](#)].
- [104] T. Papanikolaou, V. Vennin and D. Langlois, *Gravitational waves from a universe filled with primordial black holes*, *JCAP* **03** (2021) 053 [[2010.11573](#)].
- [105] D. Borah, S. Jyoti Das, R. Samanta and F.R. Urban, *PBH-infused seesaw origin of matter and unique gravitational waves*, *JHEP* **03** (2023) 127 [[2211.15726](#)].
- [106] A. Arbey and J. Auffinger, *BlackHawk: A public code for calculating the Hawking evaporation spectra of any black hole distribution*, *Eur. Phys. J. C* **79** (2019) 693 [[1905.04268](#)].
- [107] A. Arbey and J. Auffinger, *Physics Beyond the Standard Model with BlackHawk v2.0*, *Eur. Phys. J. C* **81** (2021) 910 [[2108.02737](#)].
- [108] KM3NET collaboration, *Observation of an ultra-high-energy cosmic neutrino with KM3NeT*, *Nature* **638** (2025) 376.
- [109] KM3NET collaboration, *On the Potential Galactic Origin of the Ultra-High-Energy Event KM3-230213A*, [2502.08387](#).
- [110] KM3NET collaboration, *On the potential cosmogenic origin of the ultra-high-energy event KM3-230213A*, [2502.08508](#).

- [111] A. Boccia and F. Iocco, *A strike of luck: could the KM3-230213A event be caused by an evaporating primordial black hole?*, [2502.19245](#).
- [112] D. Borah, N. Das, N. Okada and P. Sarmah, *Possible origin of the KM3-230213A neutrino event from dark matter decay*, [2503.00097](#).
- [113] K. Kohri, P.K. Paul and N. Sahu, *Super heavy dark matter origin of the PeV neutrino event: KM3-230213A*, [2503.04464](#).
- [114] J.F. Navarro, C.S. Frenk and S.D.M. White, *A Universal density profile from hierarchical clustering*, *Astrophys. J.* **490** (1997) 493 [[astro-ph/9611107](#)].
- [115] K. Akita, G. Lambiase, M. Niibo and M. Yamaguchi, *Neutrino lines from MeV dark matter annihilation and decay in JUNO*, *JCAP* **10** (2022) 097 [[2206.06755](#)].
- [116] C. Blanco and D. Hooper, *Constraints on Decaying Dark Matter from the Isotropic Gamma-Ray Background*, *JCAP* **03** (2019) 019 [[1811.05988](#)].
- [117] C.W. Bauer, N.L. Rodd and B.R. Webber, *Dark matter spectra from the electroweak to the Planck scale*, *JHEP* **06** (2021) 121 [[2007.15001](#)].
- [118] ICECUBE collaboration, *The IceCube high-energy starting event sample: Description and flux characterization with 7.5 years of data*, *Phys. Rev. D* **104** (2021) 022002 [[2011.03545](#)].
- [119] ICECUBE collaboration, *Differential limit on the extremely-high-energy cosmic neutrino flux in the presence of astrophysical background from nine years of IceCube data*, *Phys. Rev. D* **98** (2018) 062003 [[1807.01820](#)].
- [120] ICECUBE collaboration, *A search for extremely-high-energy neutrinos and first constraints on the ultra-high-energy cosmic-ray proton fraction with IceCube*, [2502.01963](#).